Probing the Anomalous Top-Yukawa Coupling at the LHC

Chih-Ting Lu (NTHU)
National Tsing Hua University, Hsinchu, Taiwan

1st IBS-Honam Focus Program on Particle Physics Phenomenology

Higgs Phenomenology 2016

- Collaborators for this work :
- Prof. Kingman Cheung
- Prof. Jae Sik Lee
- Dr. Jung Chang
- Ref : arXiv:1403.2053 JHEP 1405 (2014) 062

  arXiv:1607.06566

Outline

- 1. Motivation
- 2. Highlight some experimental results for the Higgs boson at the LHC
- 3. Formalism and Results from Higgs Precision (Higgcision) analysis
- 4. Entangling Higgs production associated with a single top and a top-pair in the presence of anomalous top-Yukawa coupling
- 5. Conclusions

Motivation

- Why is it important for the discovery of the Higgs boson ?
- 1. It is a byproduct of the BEH mechanism, so if we discover the Higgs boson, then we can confirm the BEH mechanism ! (It is NOT just a new scalar particle !)
- 2. New type of interactions :

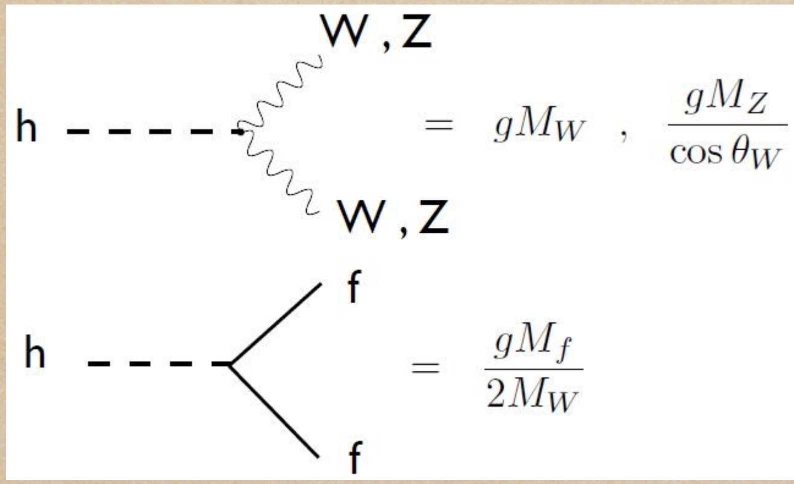

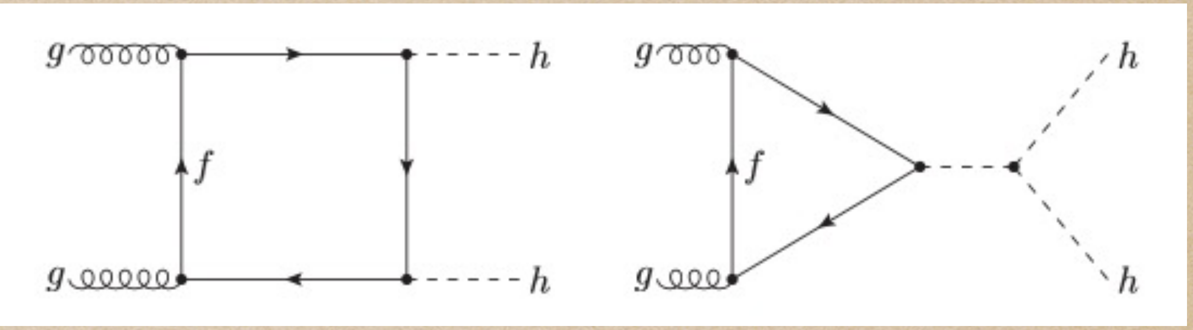

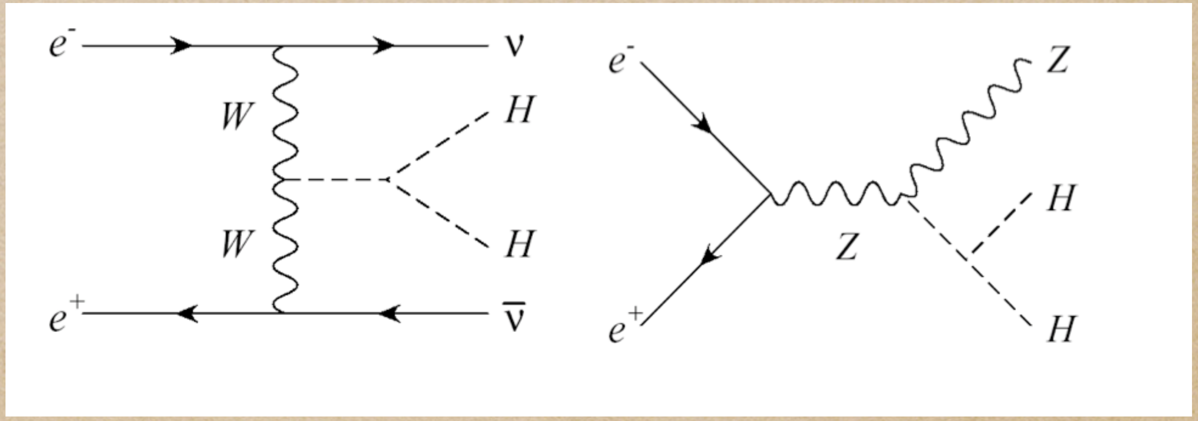

Highlight some experimental results for the Higgs boson at the LHC

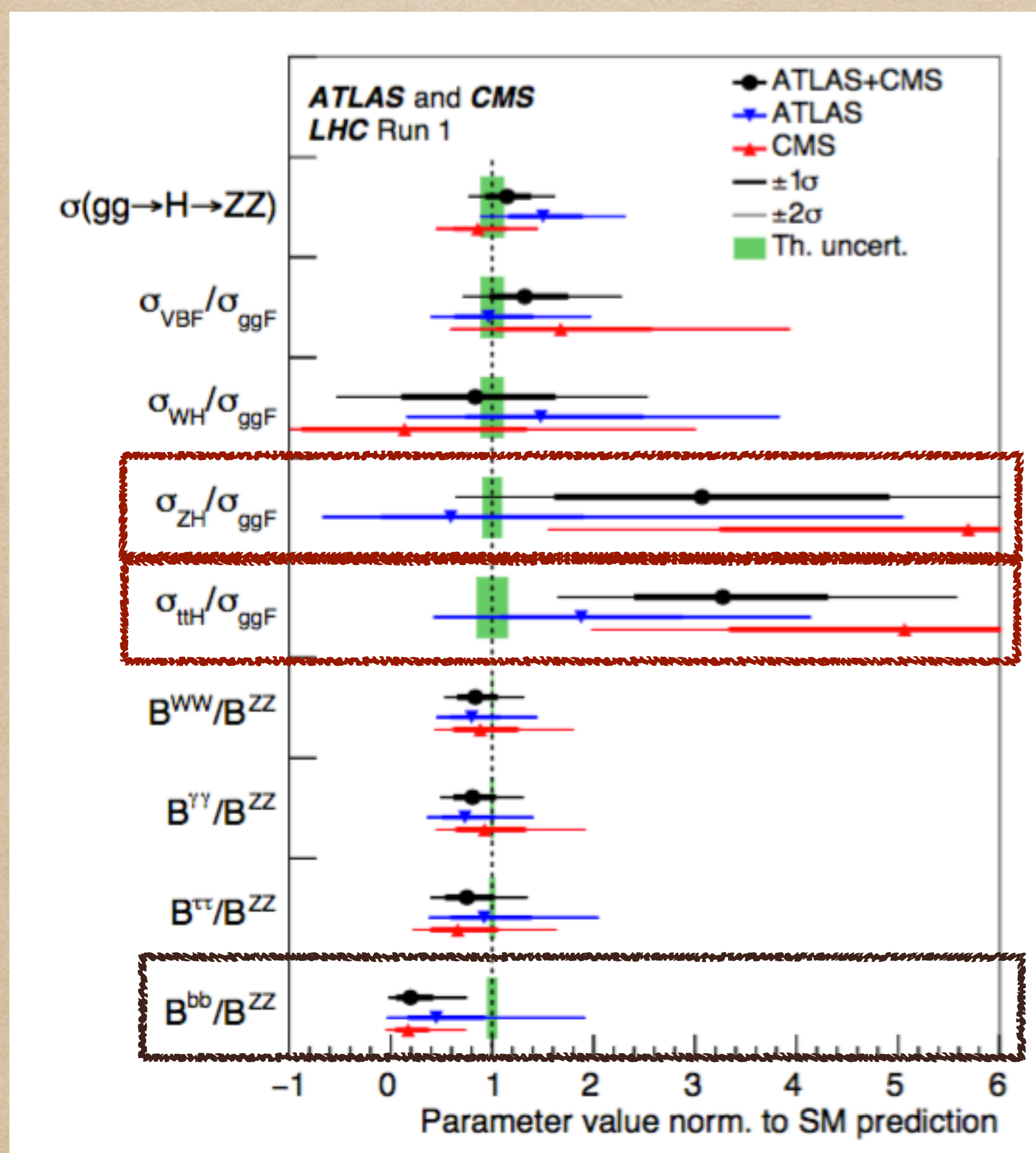

arXiv:1606.02266

$$\frac{\sigma_{ttH}/\sigma_{ggF}}{\text{the same ratio in SM}} = 3.3 \pm 0.9$$

$$\frac{\sigma_{ZH}/\sigma_{ggF}}{\text{the same ratio in SM}} = 3.2 \pm 1.4$$

$$\frac{B^{bb}/B^{ZZ}}{\text{the same ratio in SM}} = 0.19 \pm 0.21$$

Highlight some experimental results for the Higgs boson at the LHC

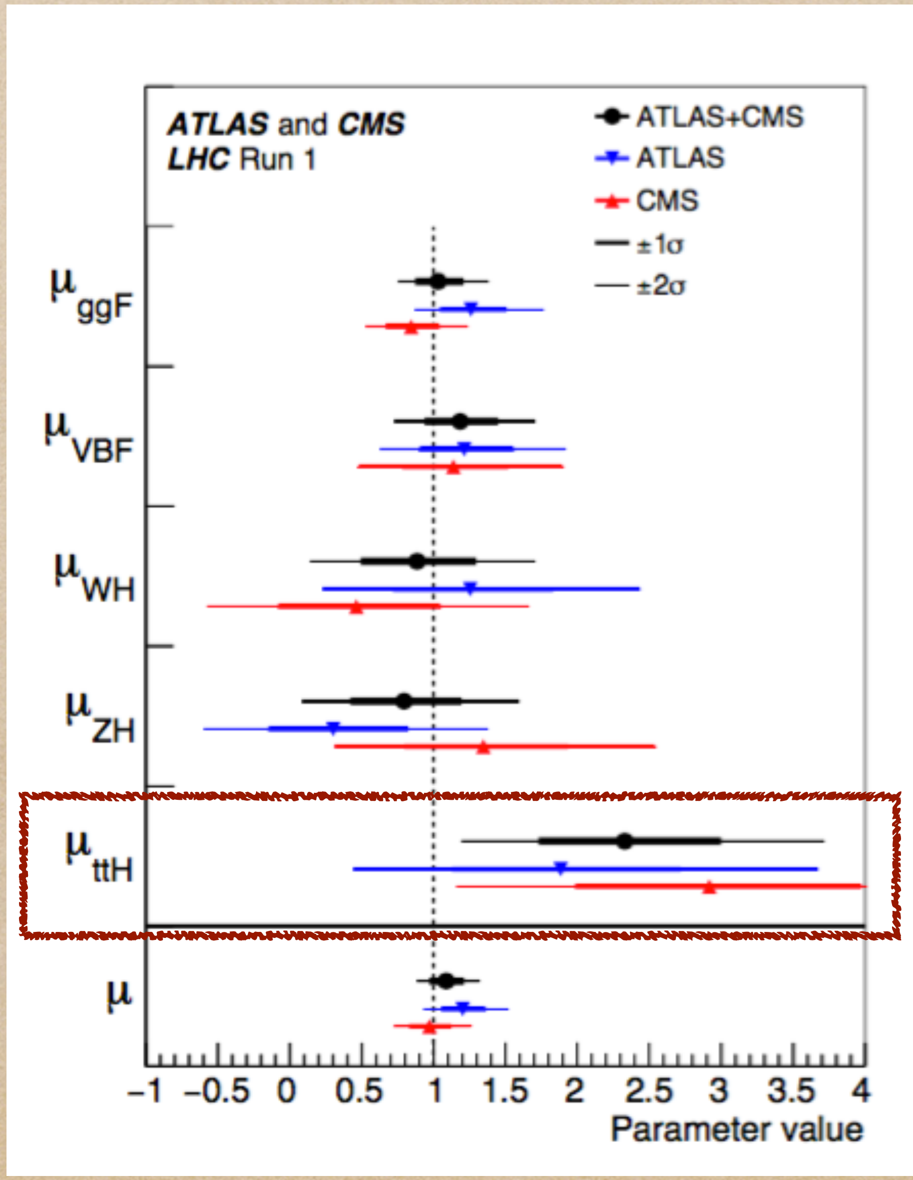

arXiv:1606.02266

Highlight some experimental results for the Higgs boson at the LHC

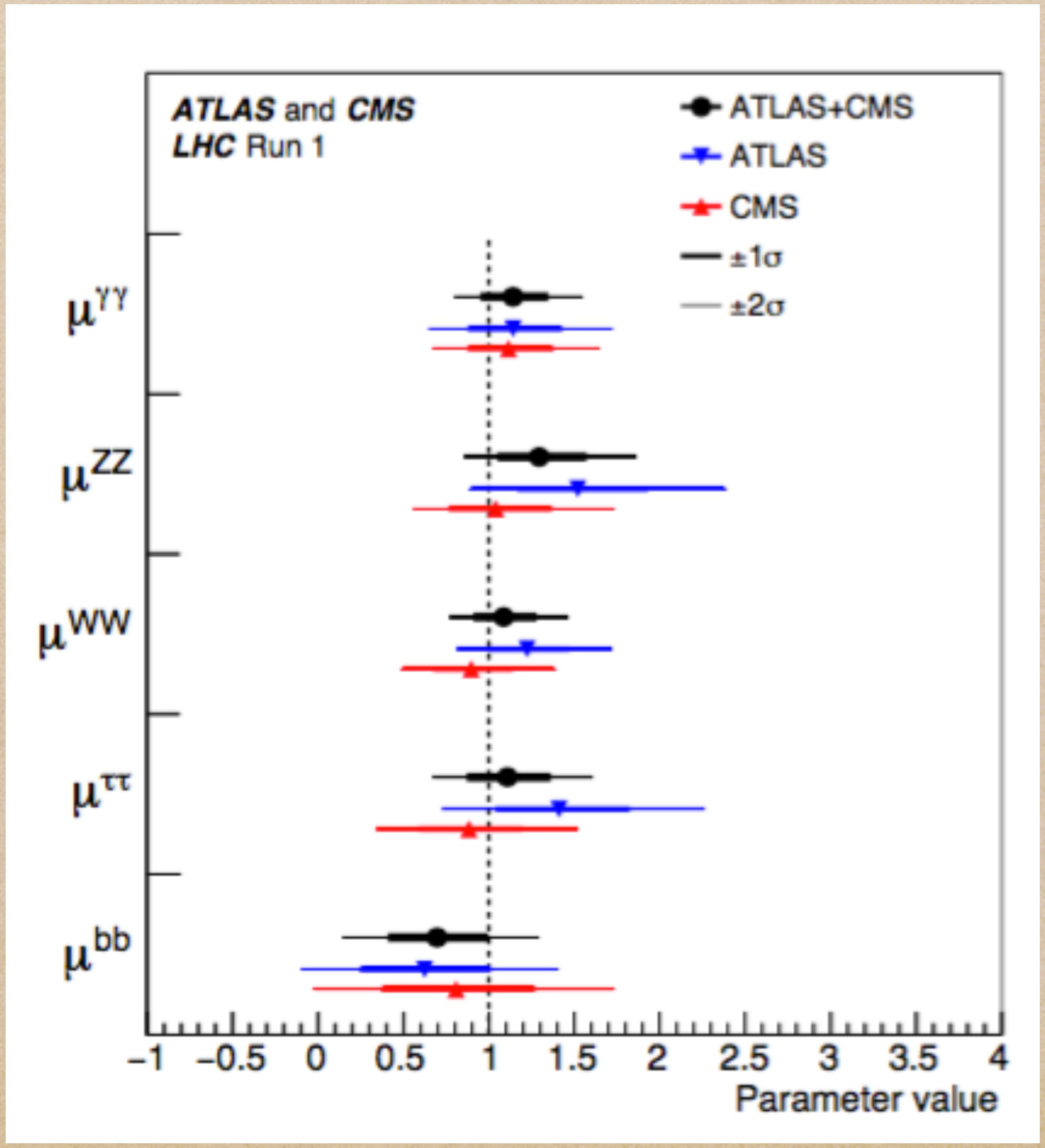

arXiv:1606.02266

Highlight some experimental results for the Higgs boson at the LHC

ttH production

Important to study directly the coupling of top to Higgs

Looking for final states with H decay to ZZ,WW and $\tau\tau$ (yielding events with 2-3 leptons).

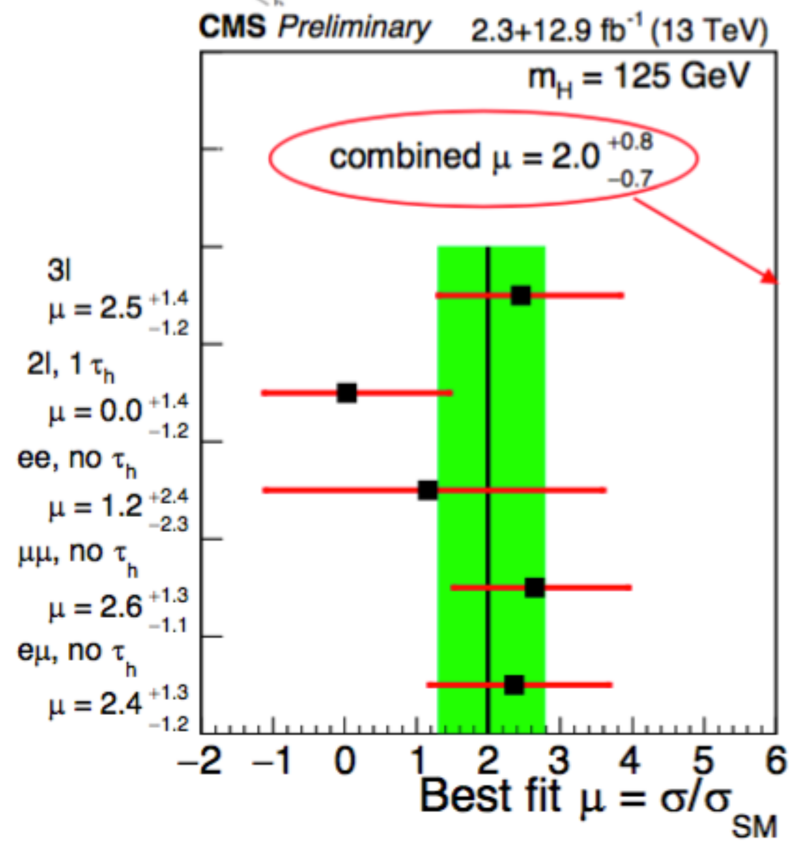

$\mu=2.0^{+0.8}{}_{-0.7}$ within statistics, compatible with SM

Highlight some experimental results for the Higgs boson at the LHC

Search for ttH production

Direct probe of top Yukawa coupling
Cross-section at 13 TeV ~4 times that at 8 TeV
Results presented with 2015+2016 data for
- ttH, H→bb
- ttH, multilepton final states (contributions from several decay chains)
- ttH, H→γγ through H→γγ event categorisation

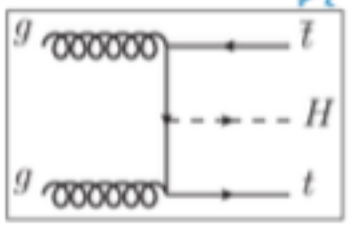

ttH combination

Combine all three 13 TeV analyses

Signal strength μ expressed relative to SM expectation

Observed significance
2.8σ (expect 1.8σ)
Cf Run-1 expected 1.5σ

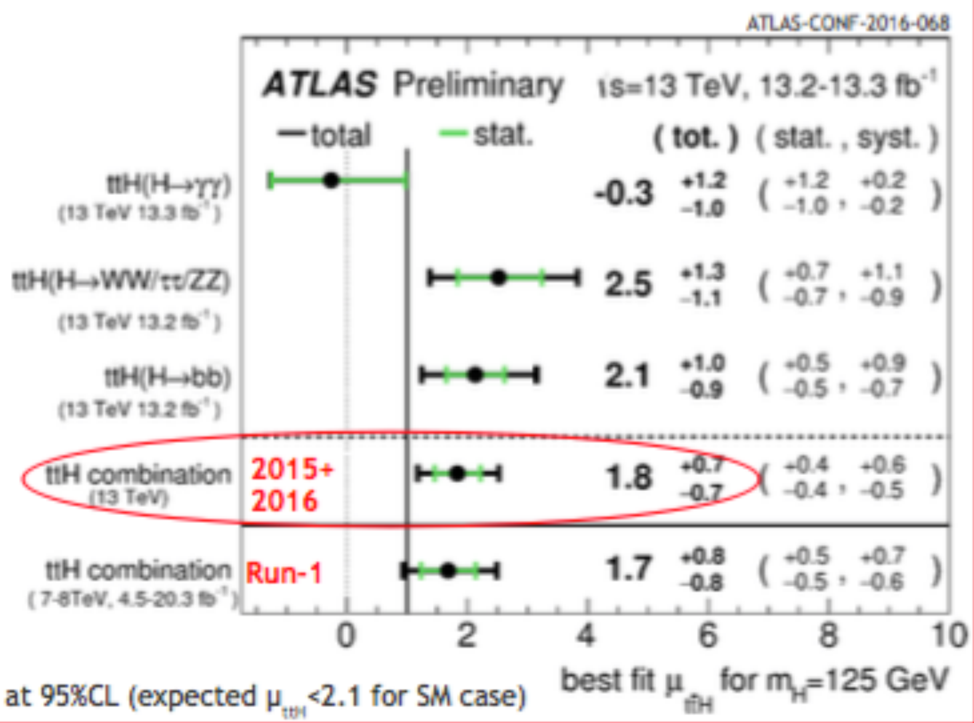

Upper limit on signal strength: $\mu_{ttH}<3.0$ at 95%CL (expected $\mu_{ttH}<2.1$ for SM case)

Formalism from Higgs Precision (Higgscision) analysis

- Assuming that the Higgs boson h is a generic CP-mixed state, we can write the gauge-Higgs and Yukawa coupling as

$$
\begin{aligned}
\mathcal{L}_{hVV} &= g m_W \left(g_{hWW} W^+_\mu W^{-\mu} + g_{hZZ} \frac{1}{2c_W^2} Z_\mu Z^\mu \right) h \,, \\
\mathcal{L}_{hff} &= - \sum_{f=t,b,c,\tau} \frac{g m_f}{2 m_W} \bar{f} \left(g^S_{hff} + i g^P_{hff} \gamma_5 \right) f \, h \,.
\end{aligned}
$$

We note $g_{hWW} = g_{hZZ} = g^S_{hff} = 1$ and $g^P_{hff} = 0$ in the SM.

Formalism from Higgs Precision (Higgscision) analysis

The amplitude for the decay process $h \to \gamma\gamma$ can be written as

$$\mathcal{M}_{h\gamma\gamma} = -\frac{\alpha m_h^2}{4\pi\, v}\left\{S^\gamma(m_h)\ (\epsilon_{1\perp}^* \cdot \epsilon_{2\perp}^*) - P^\gamma(m_h)\frac{2}{m_h^2}\langle\epsilon_1^*\epsilon_2^* k_1 k_2\rangle\right\},$$

where $k_{1,2}$ are the momenta of the two photons and $\epsilon_{1,2}$ the wave vectors of the corresponding photons, $\epsilon_{1\perp}^\mu = \epsilon_1^\mu - 2k_1^\mu(k_2\cdot\epsilon_1)/m_h^2$, $\epsilon_{2\perp}^\mu = \epsilon_2^\mu - 2k_2^\mu(k_1\cdot\epsilon_2)/m_h^2$ and $\langle\epsilon_1\epsilon_2 k_1 k_2\rangle \equiv \epsilon_{\mu\nu\rho\sigma}\,\epsilon_1^\mu\epsilon_2^\nu k_1^\rho k_2^\sigma$. Retaining only the dominant loop contributions from the third–generation fermions and $W^\pm$, and including some additional loop contributions from new particles, the scalar and pseudoscalar form factors are given by

$$S^\gamma(m_h) = 2\sum_{f=b,t,\tau} N_C\, Q_f^2\, g_{hff}^S\, F_{sf}(\tau_f) - g_{hWW} F_1(\tau_W) + \Delta S^\gamma\,,$$
$$P^\gamma(m_h) = 2\sum_{f=b,t,\tau} N_C\, Q_f^2\, g_{hff}^P\, F_{pf}(\tau_f) + \Delta P^\gamma\,, \qquad (4)$$

where $\tau_x = m_h^2/4m_x^2$, $N_C = 3$ for quarks and $N_C = 1$ for tau leptons, respectively.

In the SM, $P^\gamma = 0$, $g_{hff}^S = g_{hWW} = 1$ and $\Delta S^\gamma = 0$.

Formalism from Higgs Precision (Higgscision) analysis

Similarly, the amplitude for the decay process $h \to gg$ can be written as

$$\mathcal{M}_{Hgg} = -\frac{\alpha_s\, m_h^2\, \delta^{ab}}{4\pi\, v}\left\{S^g(m_h)\,(\epsilon^*_{1\perp}\cdot\epsilon^*_{2\perp}) - P^g(m_h)\frac{2}{m_h^2}\langle\epsilon^*_1\epsilon^*_2 k_1 k_2\rangle\right\},$$

where a and b ($a, b = 1$ to 8) are indices of the eight $SU(3)$ generators in the adjoint representation. Including some additional loop contributions from new particles, the scalar and pseudoscalar form factors are given by

$$S^g(m_h) = \sum_{f=b,t} g^S_{hff}\, F_{sf}(\tau_f) + \Delta S^g\,,$$
$$P^g(m_h) = \sum_{f=b,t} g^P_{hff}\, F_{pf}(\tau_f) + \Delta P^g\,. \tag{6}$$

In the SM, $P^g = 0$, $g^S_{hff} = 1$ and $\Delta S^g = 0$.

Formalism from Higgs Precision (Higgscision) analysis

- Since we are primarily interested in size of the gauge-Higgs and top-Yukawa couplings and the relative sign between them, for bookkeeping purpose, we use the following simplified notations

$$C_v \equiv g_{hWW} = g_{hZZ}\,, \qquad C_t^{S,P} \equiv g_{htt}^{S,P}\,, \qquad C_b^{S,P} \equiv g_{hbb}^{S,P}\,.$$

Results from Higgs Precision (Higgscision) analysis for Run-I data

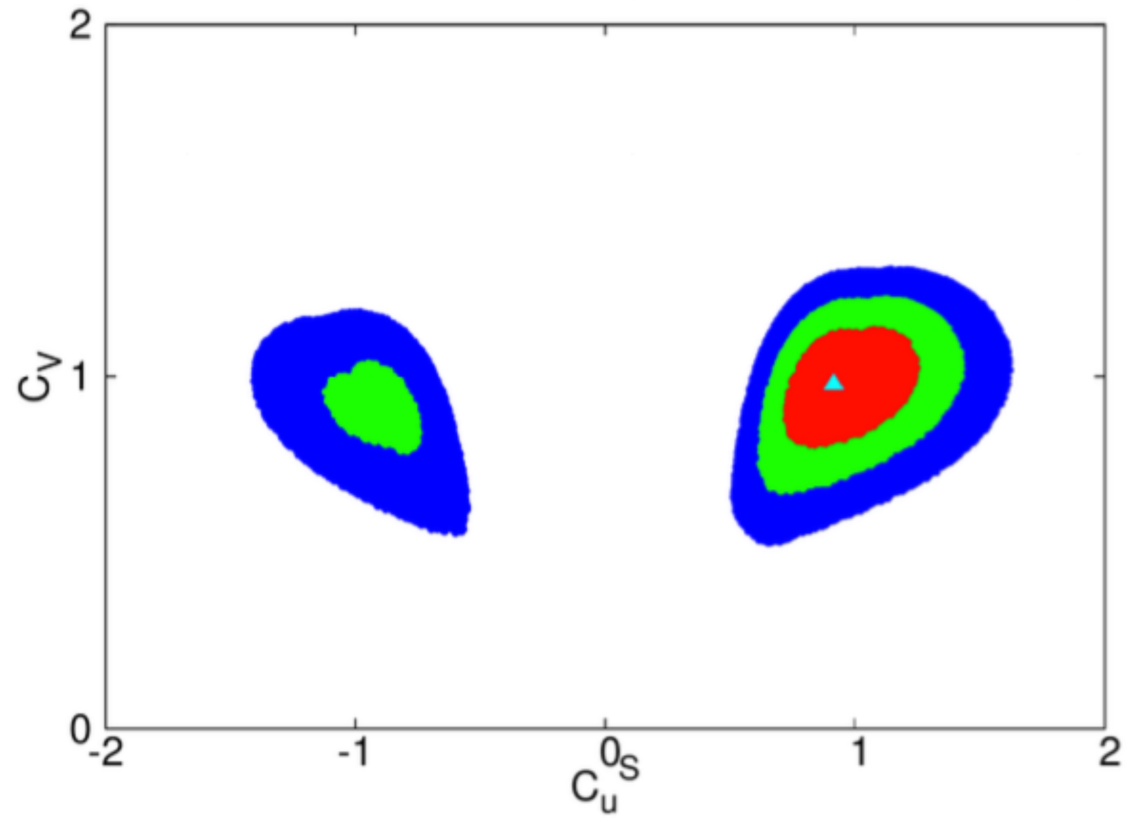

arXiv:1407.8236

Phys.Rev. D90 (2014) 095009

FIG. 2. The confidence-level regions in the plane of (C_u^S, C_v) of the CPC4 fit by varying C_u^S, C_d^S, C_l^S, and C_v while keeping $\Delta S^\gamma = \Delta S^g = \Delta\Gamma_{\rm tot} = 0$. The contour regions shown are for $\Delta\chi^2 \leq 2.3$ (red), 5.99 (green), and 11.83 (blue) above the minimum, which correspond to confidence levels of 68.3%, 95%, and 99.7%, respectively. The best-fit point is denoted by the triangle.

Results from Higgs Precision (Higgscision) analysis for Run-I data

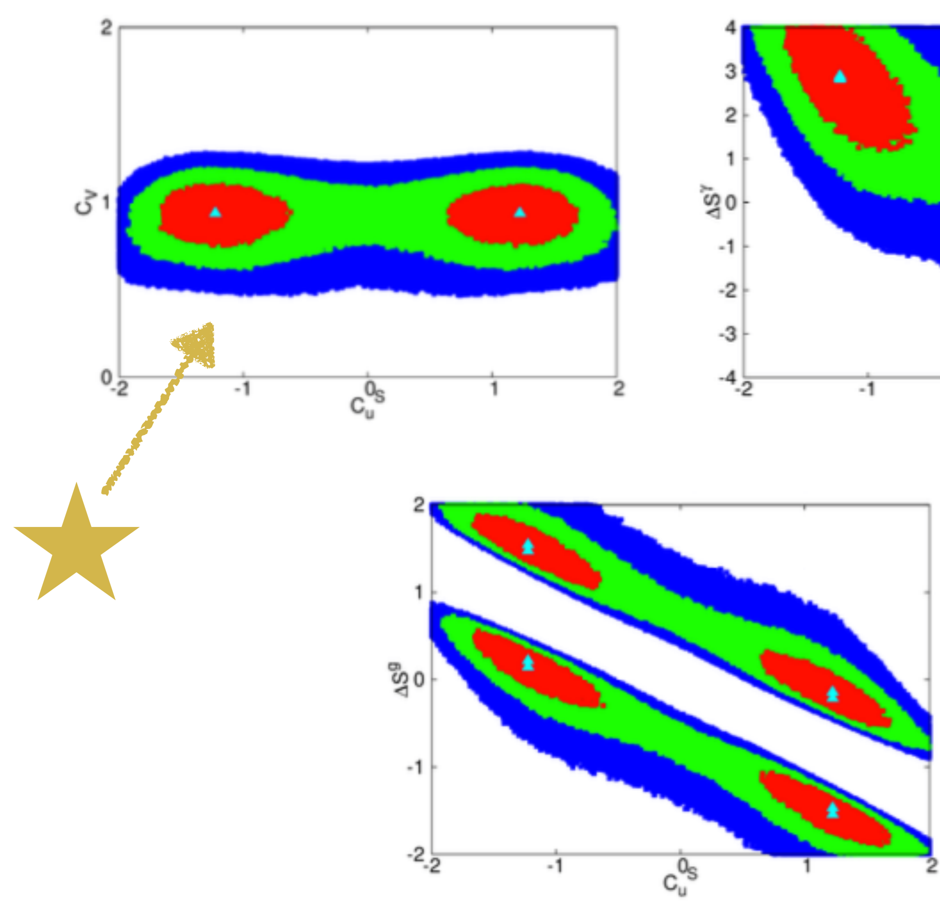

FIG. 3. The confidence-level regions in the plane of $(C_u^S,\ C_v)$, $(C_u^S,\ \Delta S^\gamma)$, an $(C_u^S,\ \Delta S^g)$ of the CPC6 fit by varying $C_u^S, C_d^S, C_l^S, C_v, \Delta S^\gamma$, and ΔS^g. The contour regions shown are for $\Delta\chi^2 \leq 2.3$ (red), 5.99 (green), and 11.83 (blue) above the minimum, which correspond to confidence levels of 68.3%, 95%, and 99.7%, respectively. The best-fit points are denoted by the triangles.

arXiv:1407.8236

Phys.Rev. D90 (2014) 095009

Results from Higgs Precision (Higgscision) analysis for Run-I data

As shown in Refs. [3] in which the model-independent fit to the current Higgs data is performed, the negative $C_t^S = -1$ is ruled at 95%CL if only the gauge-Higgs coupling C_v and the top-Yukawa coupling C_t^S vary. However, $C_t^S = -1$ is still allowed at 95%CL when the gauge-Higgs C_v, top-Yukawa C_t^S, bottom-Yukawa C_b^S, and tau-Yukawa C_τ^S couplings are all allowed to vary. Furthermore, if some sizable contributions to ΔS^γ and ΔS^g due to additional new particles running in the loop are assumed, a broad range of C_t^S between -2 and $+2$ is still consistent with the current Higgs data.

Results from Higgs Precision (Higgscision) analysis for Run-I data

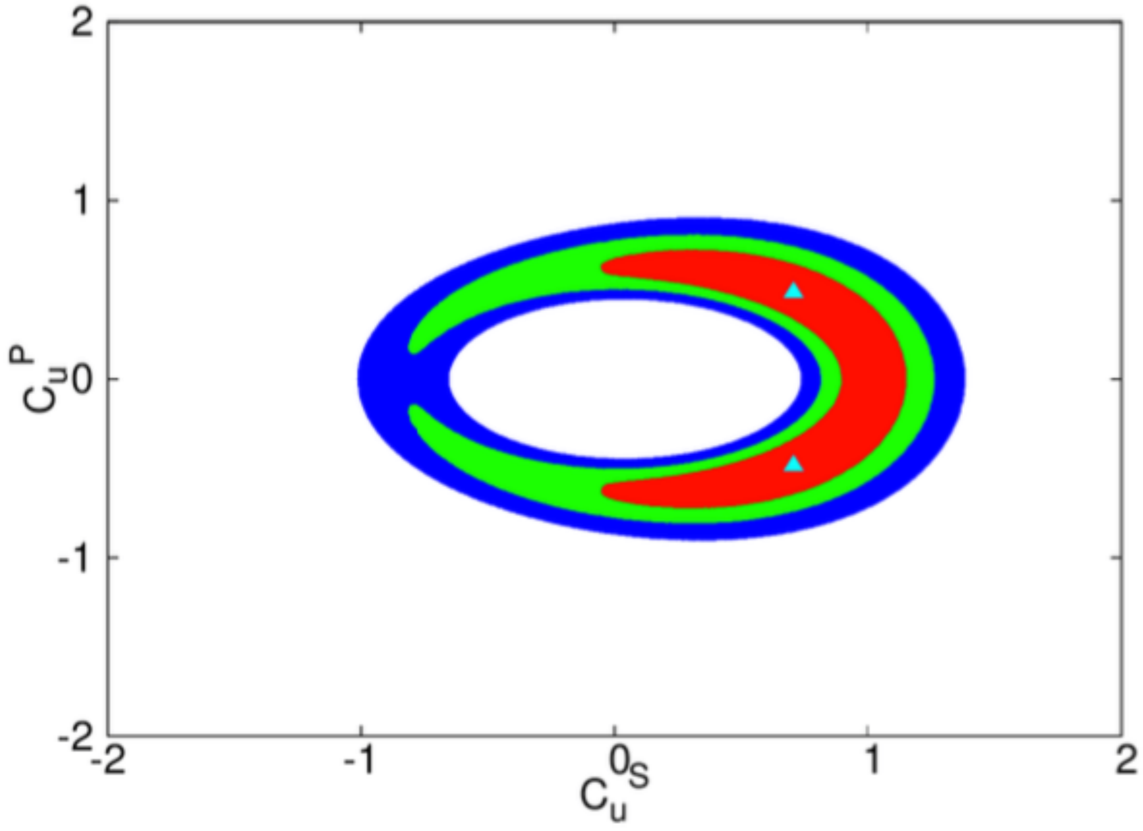

arXiv:1407.8236

Phys.Rev. D90 (2014) 095009

FIG. 4. The confidence-level regions of the fit by varying the scalar Yukawa couplings C_u^S and C_v , and the pseudoscalar Yukawa couplings C_u^P; while keeping others at the SM values. The description of contour regions is the same as in Fig. 2.

- Entangling Higgs production associated with a single top and a top-pair in the presence of anomalous top-Yukawa coupling

ttH production mode in Run-I data

It is strange …

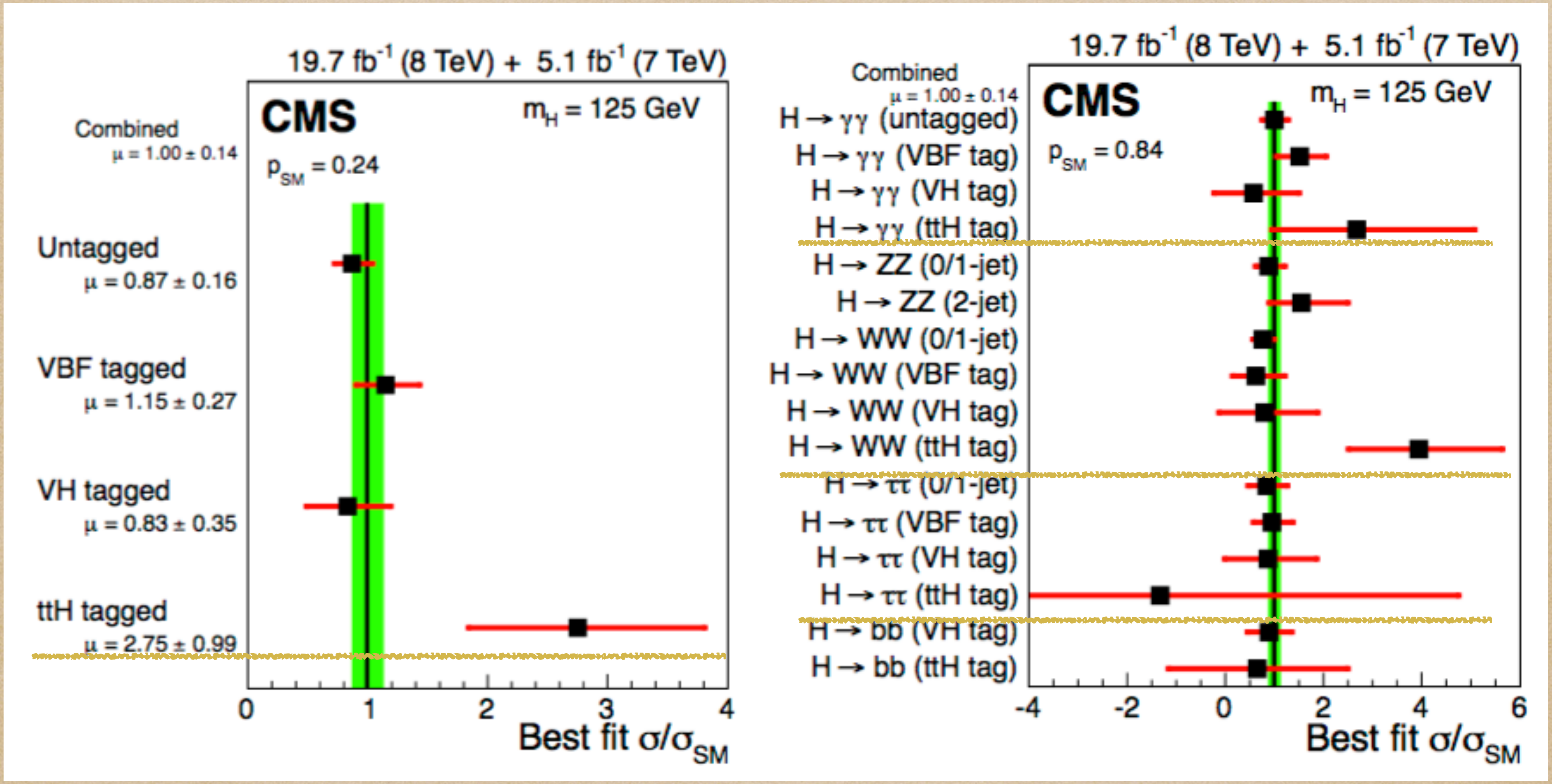

ttH production mode in Run-I data

It is strange …

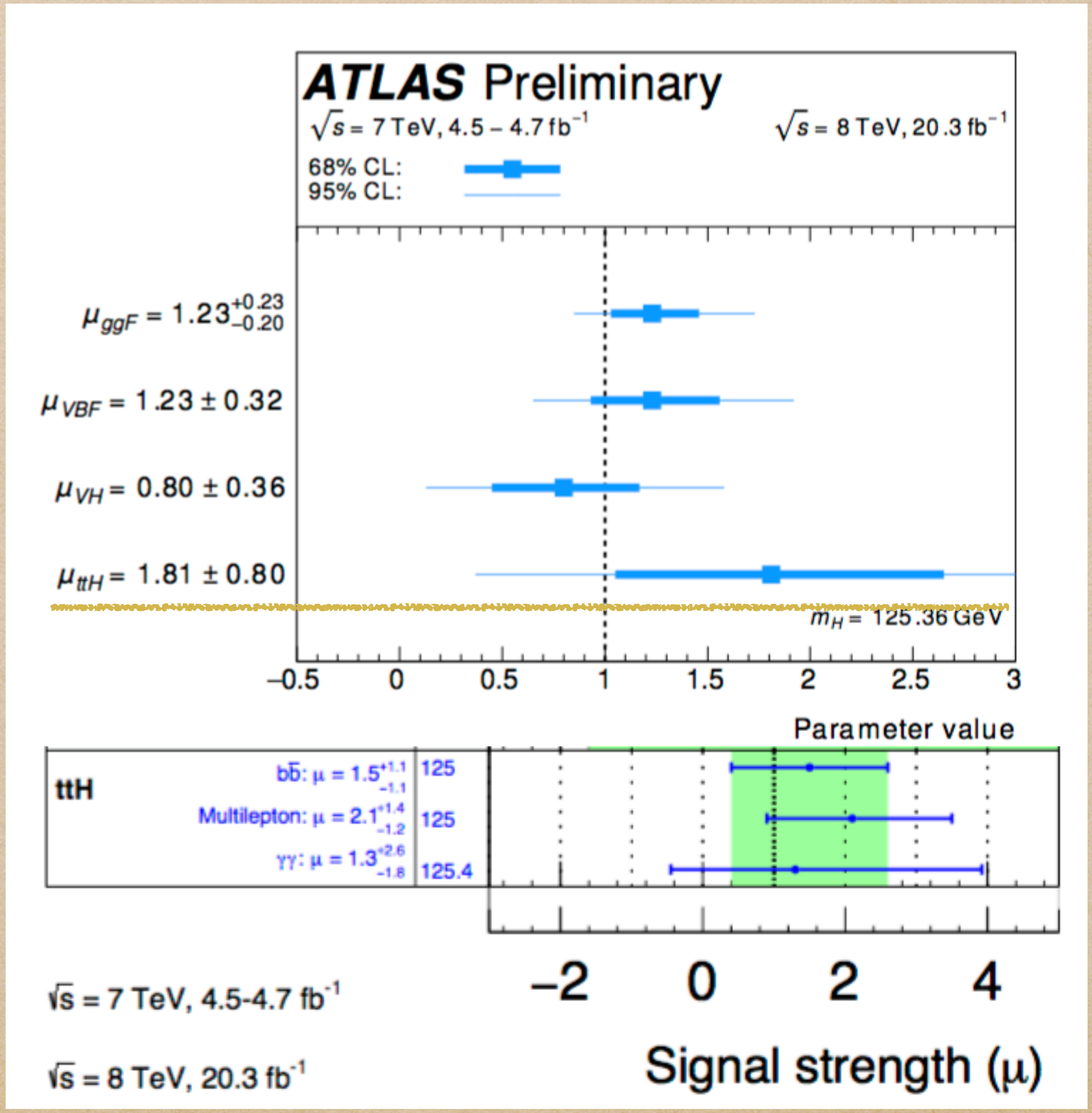

ttH production mode in Run-I data

It is strange …

TABLE I. The best-fit values for the category-dependent signal strengths $\mu_{tth}^{\rm CMS}$ and $\mu_{tth}^{\rm ATLAS}$ coming from the CMS [7] and ATLAS [10][14][15] searches, respectively, for the associated production of the Higgs boson with a top quark pair at $\sqrt{s}$= 7 and 8 TeV for m_h = 125.6 GeV (CMS) / 125 GeV (ATLAS).

	CMS $t\bar{t}h$ channel	ATLAS $t\bar{t}h$ channel
Category	$\mu_{tth}^{\rm CMS}$	$\mu_{tth}^{\rm ATLAS}$
$\gamma\gamma$	$+2.7^{+2.6}_{-1.8}$	$+1.3^{+3.3}_{-2.1}$
$b\bar{b}$	$+0.7^{+1.9}_{-1.9}$	$+1.5^{+1.1}_{-1.1}$
$\tau_h\tau_h$	$-1.3^{+6.3}_{-5.5}$	–
$2\ell 1\tau_h$	–	$-0.9^{+3.1}_{-2.0}$
$1\ell 2\tau_h$	–	$-9.6^{+9.6}_{-9.7}$
4ℓ	$-4.7^{+5.0}_{-1.3}$	$+1.8^{+6.9}_{-2.0}$
3ℓ	$+3.1^{+2.4}_{-2.0}$	$+2.8^{+2.2}_{-1.8}$
$ss2\ell$	$+5.3^{+2.1}_{-1.8}$	$+2.8^{+2.1}_{-1.9}$

Our Strategy

- In this work, we attempt to interpret the excess by exploiting the strong entanglement between the associated Higgs production with a single top quark (thX) and tth production in the presence of anomalous top-Yukawa coupling.
- As well known, tth production only depends on the absolute value of the top-Yukawa coupling.
- Meanwhile, in thX production, this degeneracy is lifted through the strong interference between the two main contributions which are proportional to the top-Yukawa and the gauge-Higgs couplings, respectively.
- Especially, when the relative sign of the top-Yukawa coupling with respect to the gauge-Higgs coupling is reversed, the thX cross section can be enhanced by more than one order of magnitude.

tth production at LO

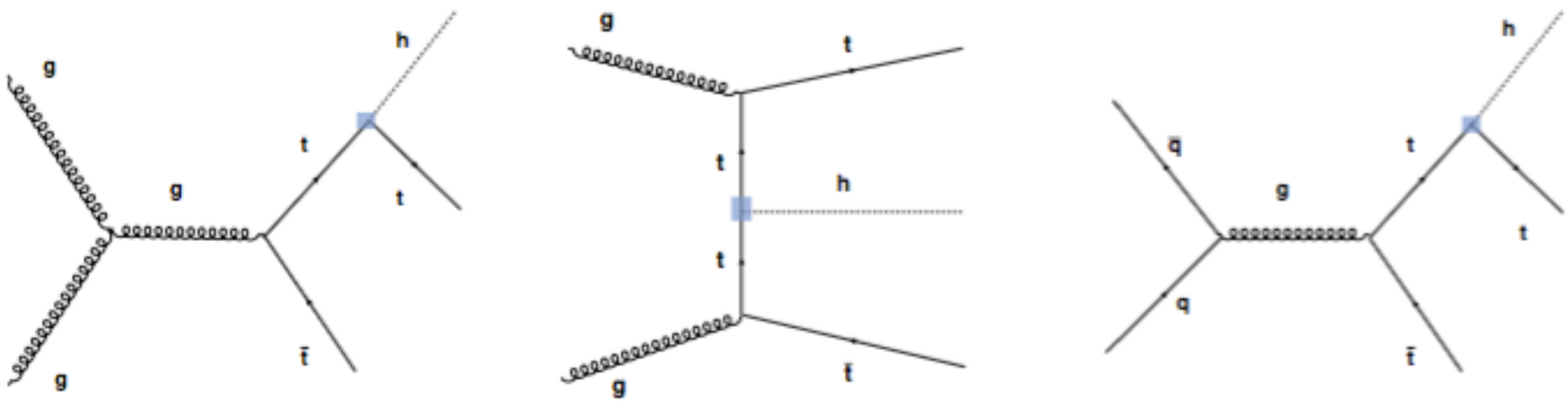

FIG. 1. Feynman diagrams contributing to $t\bar{t}h$ production at LO.

thX production with X=j

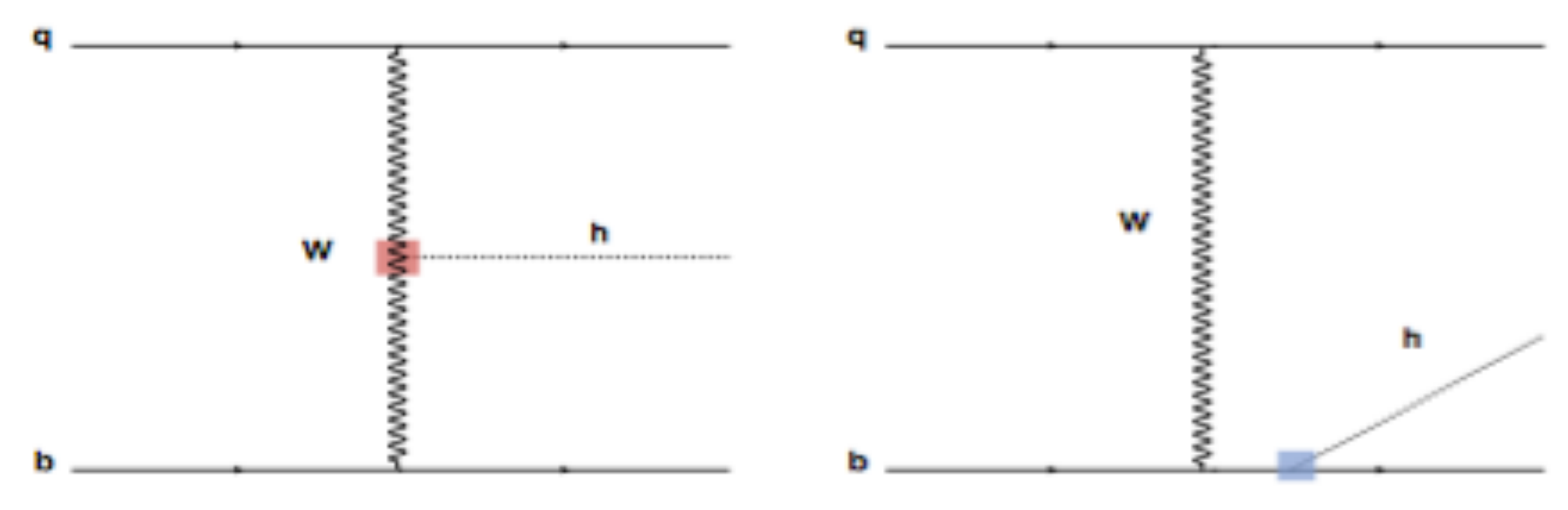

FIG. 2. Feynman diagrams contributing to thX production with $X = j$.

thX production with X=jb

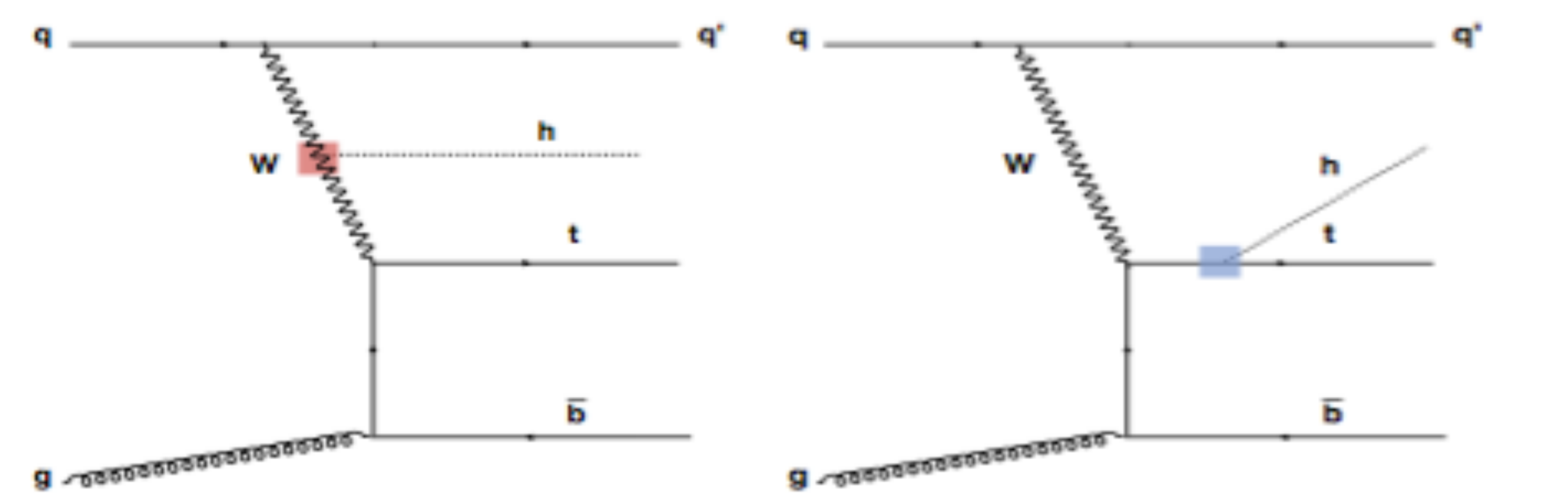

FIG. 3. Feynman diagrams contributing thX production with $X = jb$.

thX production with X=W

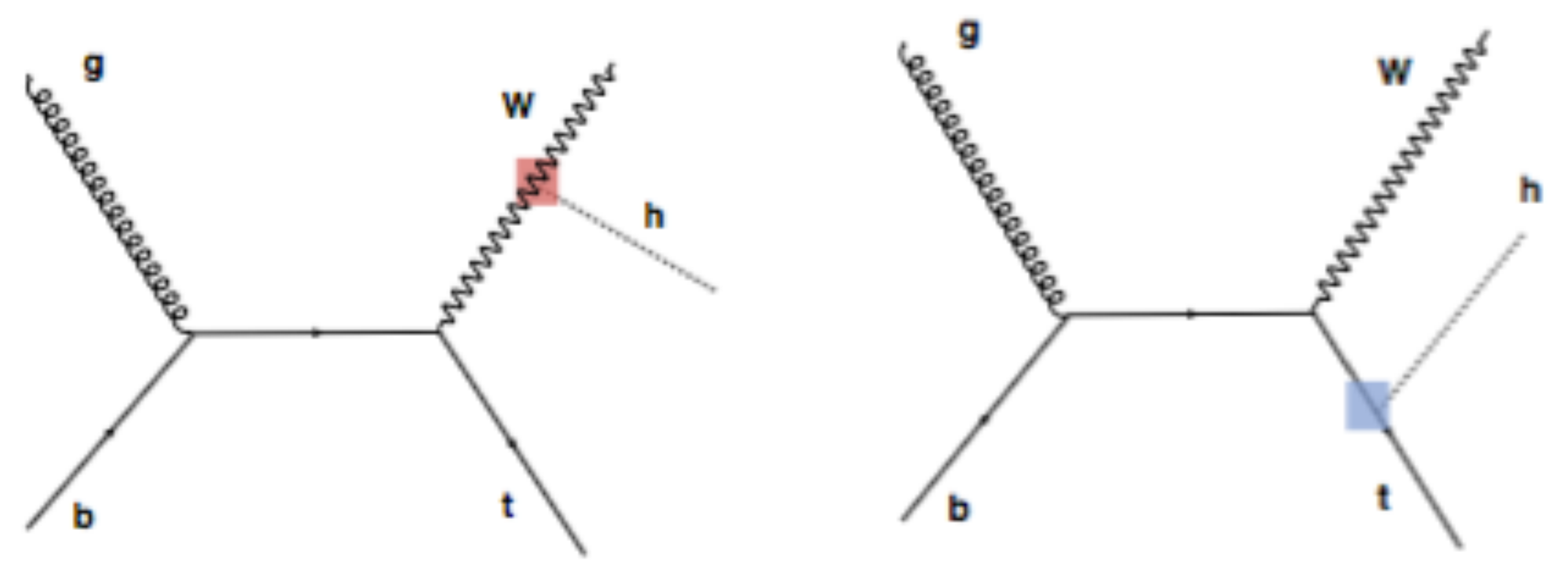

FIG. 4. Feynman diagrams contributing thX production with $X = W$.

Variation of cross sections for thX production

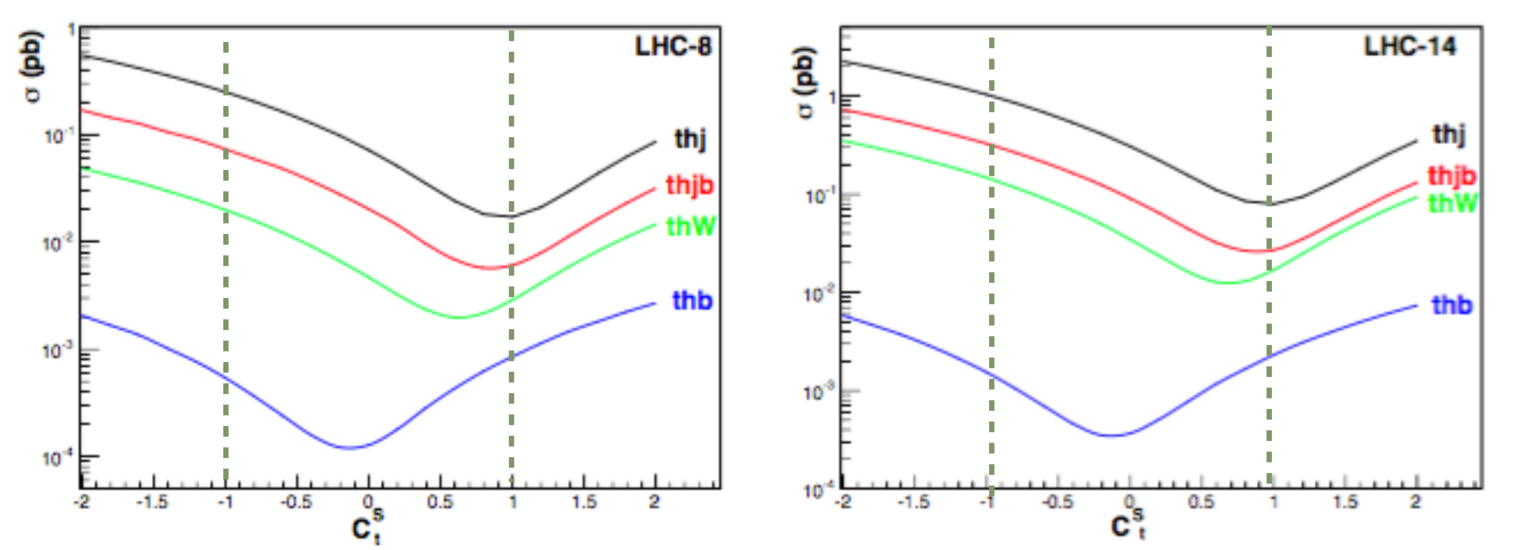

Figure 5. Variation of the total cross sections versus C_t^S for $pp \to thX$ with $X = j, jb, W, b$ in the order of the size of cross sections at (a) LHC-8 and (b) LHC-14. We have taken $C_v = C_b^S = 1$ and $C_{t,b}^P = 0$. No cuts are imposed except for the second process $pp \to thjb$ in which we applied the cuts in eq. (3.1) to remove the divergence.

	$\sigma(pp \to thX)$[fb]			
	$X = j$	$X = j + b$	$X = W$	$X = b$
$C_t^S = +1$ (SM)	79.4 (17.1)	27.1 (5.95)	17.0 (2.89)	2.32(0.833)
$C_t^S = 0$	305 (71.4)	90.0 (19.8)	34.4 (4.66)	0.368 (0.126)
$C_t^S = -1$	1030 (249)	325 (72.8)	146 (19.8)	1.52 (0.536)

Table 1. The leading-order production cross sections in fb for the processes $pp \to th + X$ at 14 TeV (8 TeV) LHC, taking $C_v = C_b^S = 1$ and $C_{t,b}^P = 0$. We have not applied any cuts except for the case with $X = j + b$ for which we required $p_{T_b} > 25$ GeV, $|\eta_b| < 2.5$; $p_{T_j} > 10$ GeV, $|\eta_j| < 5$, see text for details.

Variation of cross sections for thX production versus C^P_t

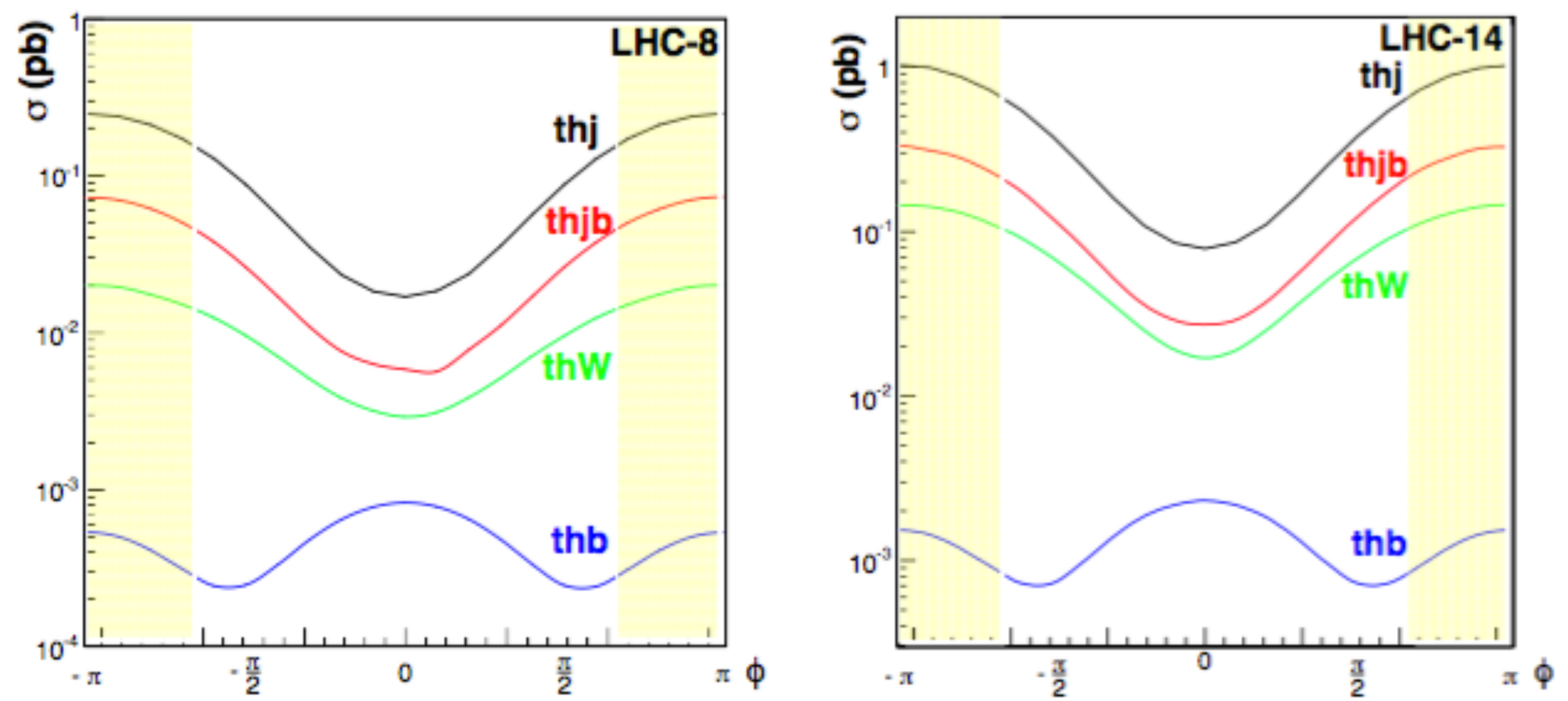

Figure 6. Production cross sections at the LHC-14 for $pp \to thj$ versus $\phi = \arctan(C_t^P/C_t^S)$ under the constraint $(C_t^S/0.86)^2 + (C_t^P/0.56)^2 = 1$. We take $C_v = 1$. The shaded regions are those disallowed at 68% C.L. by the Higgs data obtained in ref. [3].

Signal Strength

First we note that signal strengths depend on the decay modes of the top quark and the Higgs boson, as well as their production mechanisms. For a choice of experimentally-defined decay mode $\mathcal{D}$, and taking into account the thX production processes, we define the signal strength $\mu(t\bar{t}h)$ with respect to the SM $t\bar{t}h$ production as follows

$$\mu(t\bar{t}h) = \frac{\eta_1 \sigma(t\bar{t}h) B(t\bar{t}h \to \mathcal{D}) + \sum_{X=j,jb,W} \eta_X \sigma(thX) B(thX \to \mathcal{D})}{\eta_1^{\rm SM} \sigma(t\bar{t}h)_{\rm SM} B(t\bar{t}h \to \mathcal{D})_{\rm SM}}, \tag{8}$$

where $\sigma(t\bar{t}h) = \sigma(pp \to t\bar{t}h)$ and $\sigma(thX) = \sigma(pp \to thX) + \sigma(pp \to \bar{t}hX)$ are understood.

Signal Strength

The detection efficiencies η's depend on the experimental apparatuses and cuts for the specific production and decay mode. By introducing the cross-section ratios

$$R(t\bar{t}h) \equiv \frac{\sigma(t\bar{t}h)}{\sigma(t\bar{t}h)_{\rm SM}}\,, \quad R(thj) \equiv \frac{\sigma(thj)}{\sigma(t\bar{t}h)_{\rm SM}}\,,$$

$$R(thjb) \equiv \frac{\sigma(thjb)}{\sigma(t\bar{t}h)_{\rm SM}}\,, \quad R(thW) \equiv \frac{\sigma(thW)}{\sigma(t\bar{t}h)_{\rm SM}}\,, \qquad (9)$$

and the $\mathcal{D}$-dependent detection-efficiency ratios

$$\epsilon_1 \equiv \frac{\eta_1 B(t\bar{t}h \to \mathcal{D})}{\eta_1^{\rm SM} B(t\bar{t}h \to \mathcal{D})_{\rm SM}}\,, \quad \epsilon_2 \equiv \frac{\eta_j B(thj \to \mathcal{D})}{\eta_1^{\rm SM} B(t\bar{t}h \to \mathcal{D})_{\rm SM}}\,,$$

$$\epsilon_3 \equiv \frac{\eta_{jb} B(thjb \to \mathcal{D})}{\eta_1^{\rm SM} B(t\bar{t}h \to \mathcal{D})_{\rm SM}}\,, \quad \epsilon_4 \equiv \frac{\eta_W B(thW \to \mathcal{D})}{\eta_1^{\rm SM} B(t\bar{t}h \to \mathcal{D})_{\rm SM}}\,, \qquad (10)$$

one may have

$$\mu(t\bar{t}h) = \epsilon_1\, R(t\bar{t}h) + \epsilon_2\, R(thj) + \epsilon_3\, R(thjb) + \epsilon_4\, R(thW)\,. \qquad (11)$$

We note that $\epsilon_1 = R(t\bar{t}h) = 1$ in the SM limit of $C_v = 1$, $C_t^S = +1$, and $C_t^P = 0$ and $\mu(t\bar{t}h)$ is always larger than 1 due to the entanglement of thX production. Our main task is to calculate the cross section ratios R's in the presence of anomalous top-Yukawa coupling and the detection-efficiency ratios $\epsilon_{1,2,3,4}$ for various top-quark and Higgs-boson decay modes.

Signal Strength

TABLE IV. The cross-section ratios $R(t\bar{t}h)$ and $R(thX)$ with $X = j, jb, W$ defined in Eq. (9). We are taking $\sqrt{s} = 8$ TeV (LHC-8) and $C_t^S = \pm 1\,, \pm 1.5$.

LHC-8	$C_t^S = 1$	$C_t^S = -1$	$C_t^S = 1.5$	$C_t^S = -1.5$
Cross Section of $t\bar{t}h$(pb)	0.13			
$R(t\bar{t}h)$	1	1	2.25	2.25
$R(thj)$	0.16	1.86	0.30	2.82
$R(thjb)$	4.77e-2	0.59	9.39e-2	0.93
$R(thW)$	3.21e-2	0.19	7.05e-2	0.31

Categories

In the $\gamma\gamma$ category for $h \to \gamma\gamma$, both CMS [7] and ATLAS [14] included all the decay modes of a top-quark pair: semileptonic ($t\bar{t} \to l\nu jjbb$), leptonic ($t\bar{t} \to l\nu l\nu bb$), and hadronic ($t\bar{t} \to jjjjbb$) modes. On the other hand, in the $b\bar{b}$ category for $h \to b\bar{b}$, both CMS [7] and ATLAS [15] considered only the semileptonic and leptonic decay modes of the top-quark pair. Finally, in the categories of $ss2\ell$ and 3ℓ for $h \to$ multileptons, both CMS [7] and ATLAS [10] included only the semileptonic decay mode of the top-quark pair.

Category Lepton for h -> multileptons

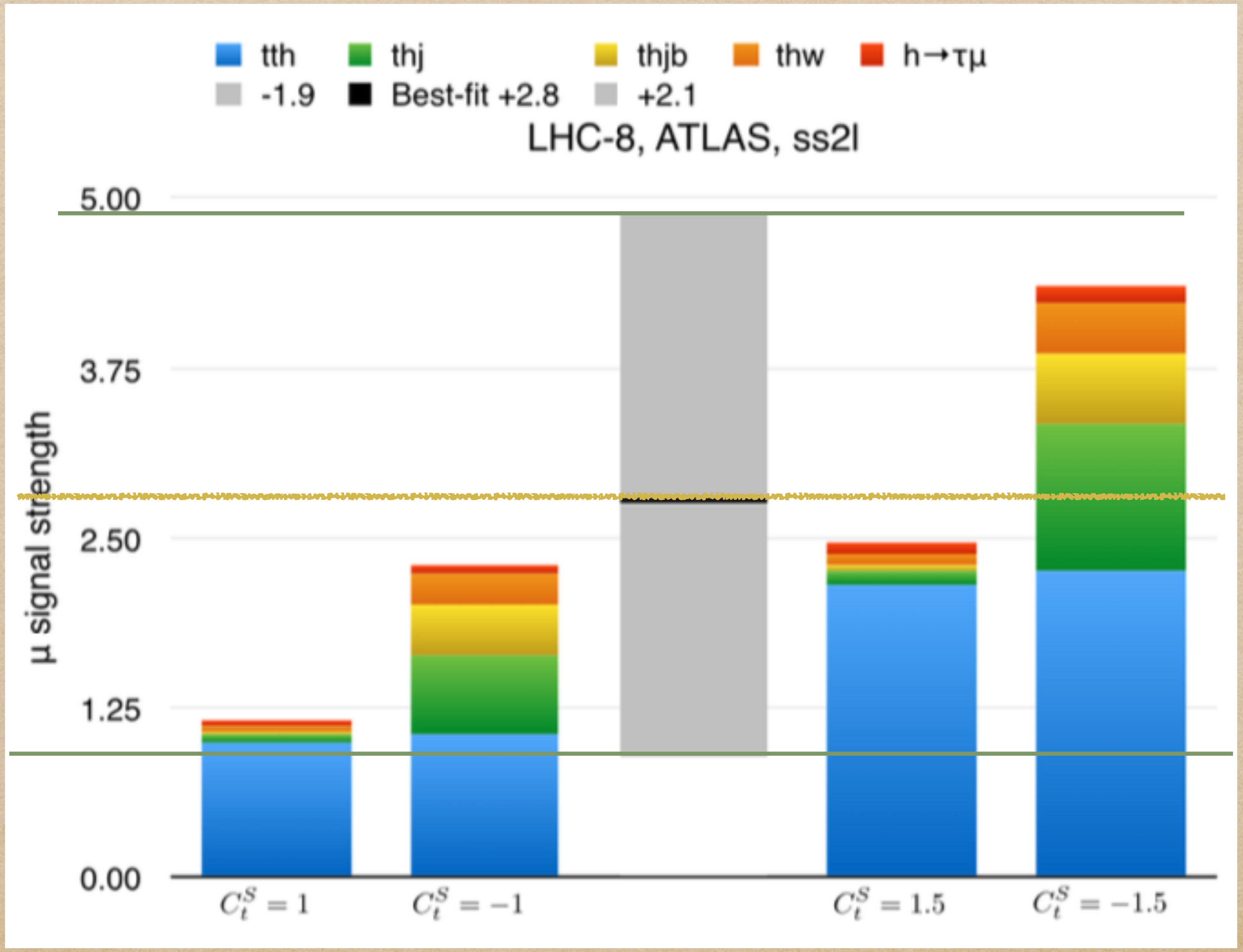

Category Lepton for h -> multileptons

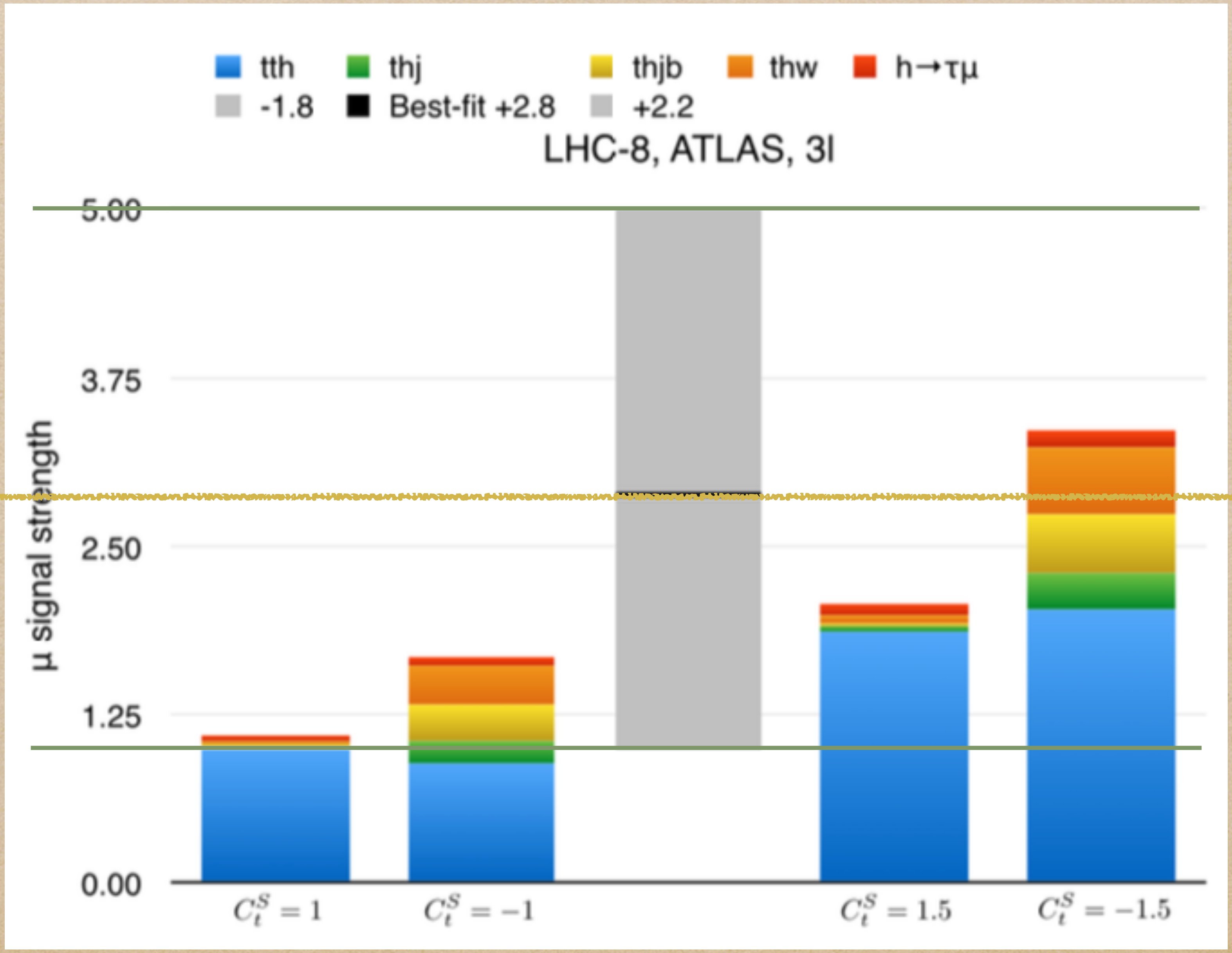

Category Lepton for h -> multileptons

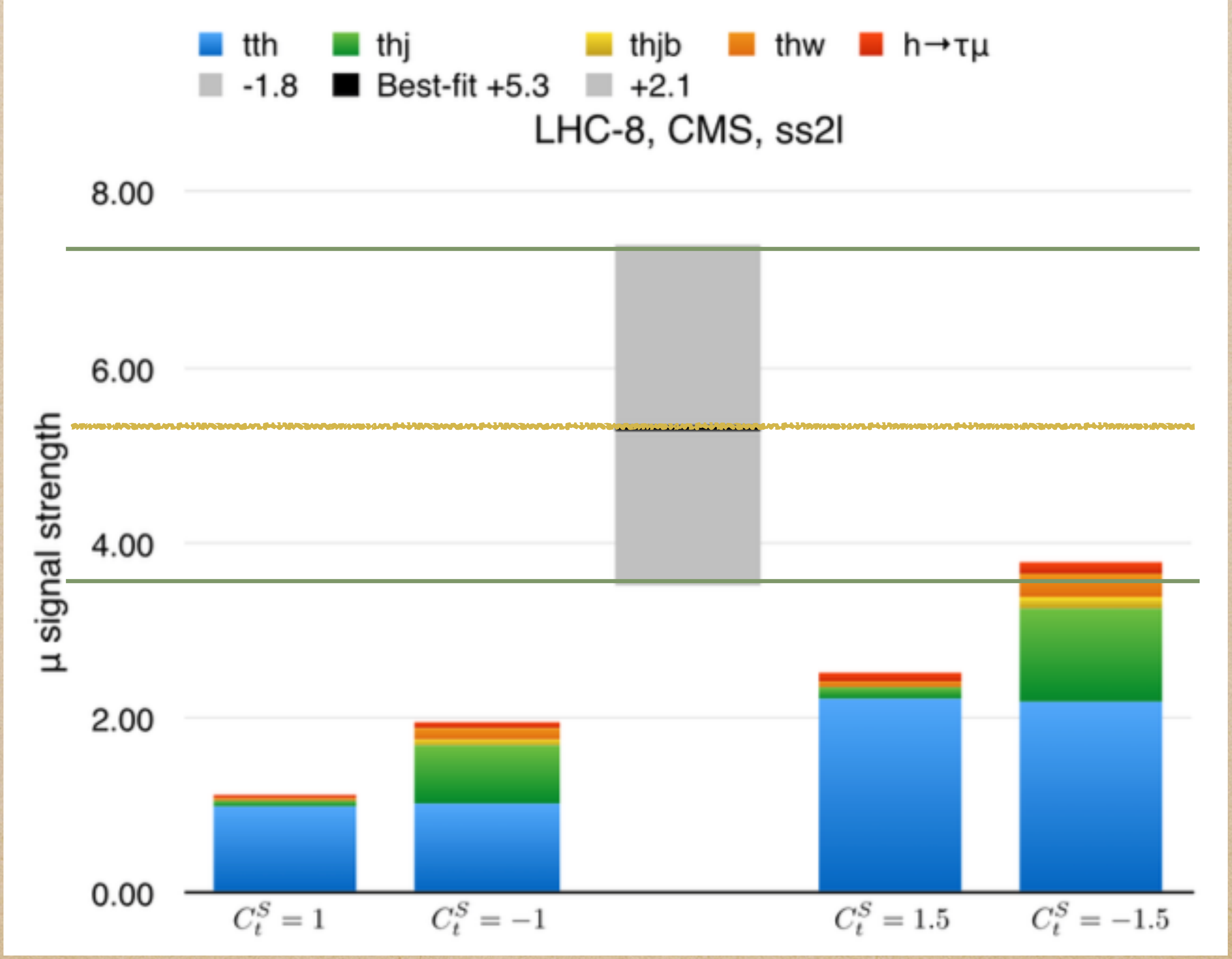

Category Lepton for h -> multileptons

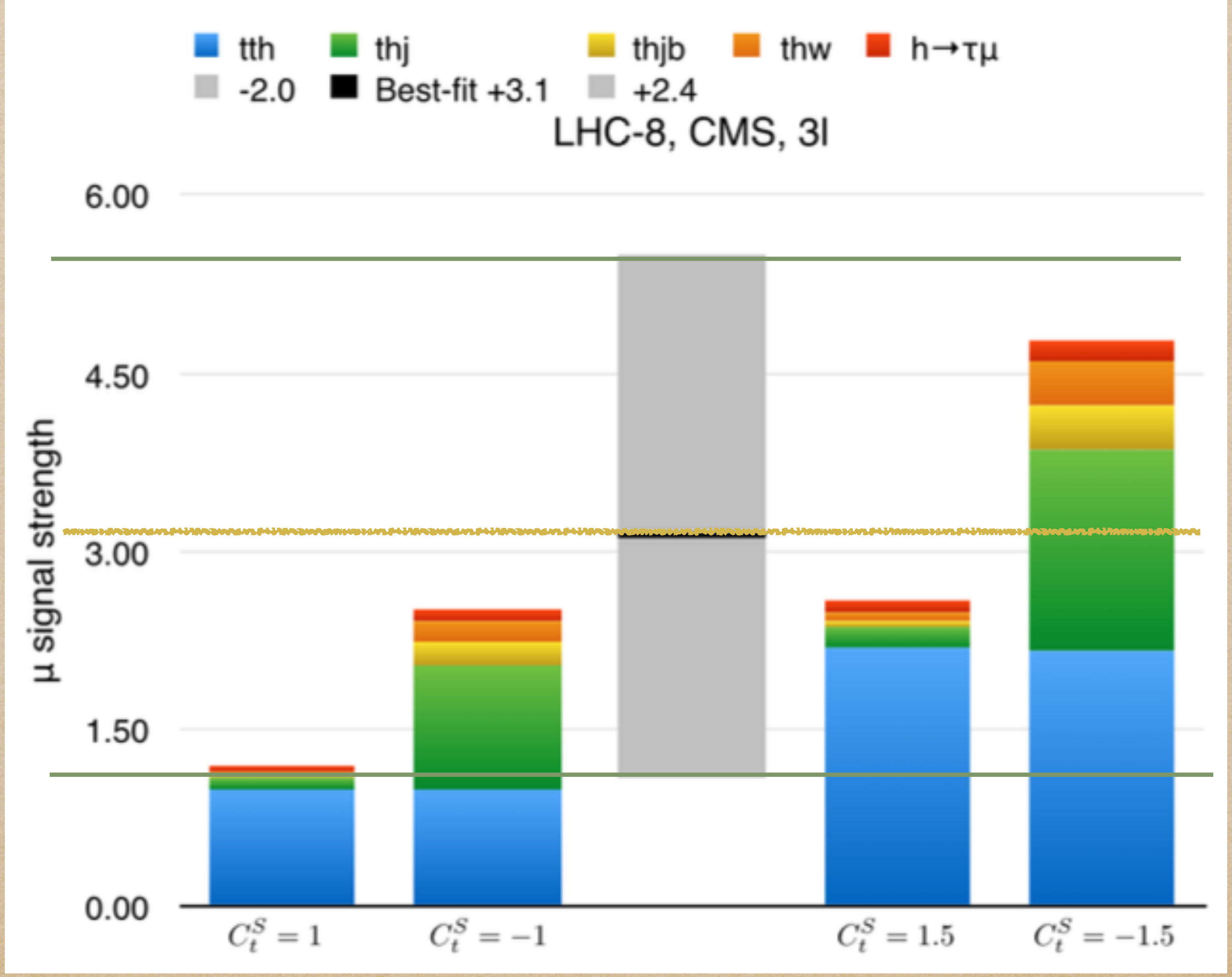

Category diphoton for h -> diphoton

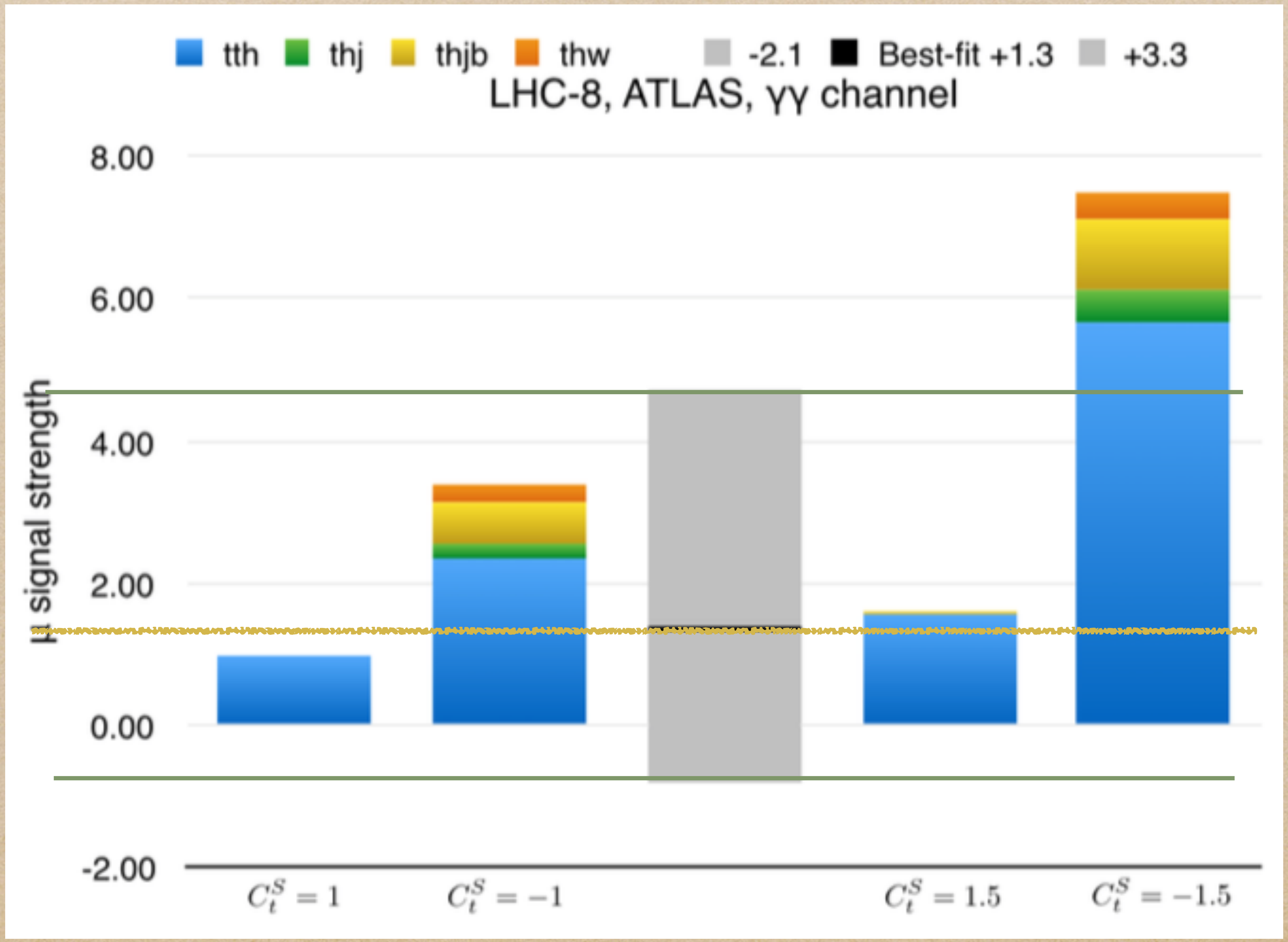

Category diphoton for h -> diphoton

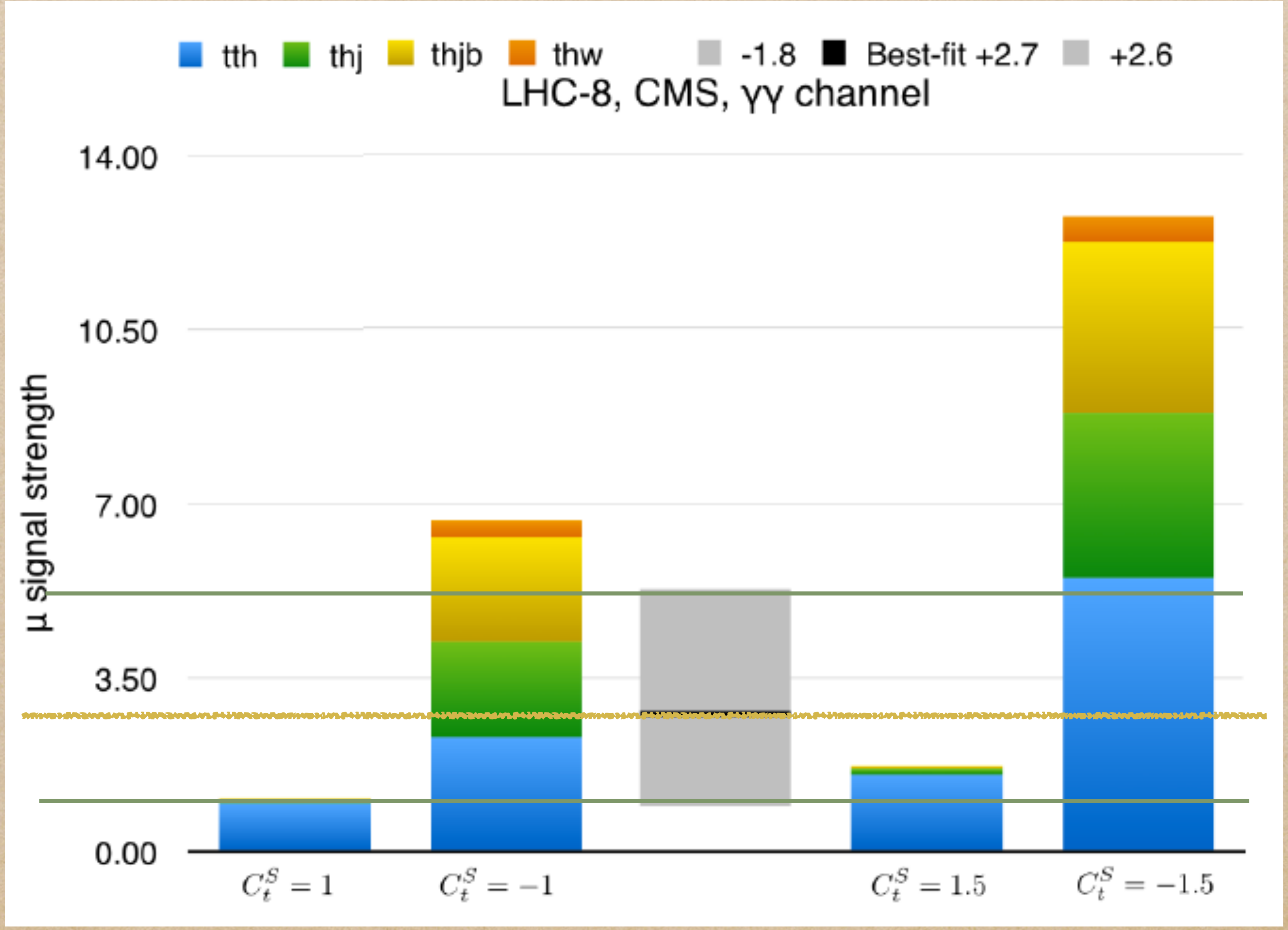

Category bb for h -> bb

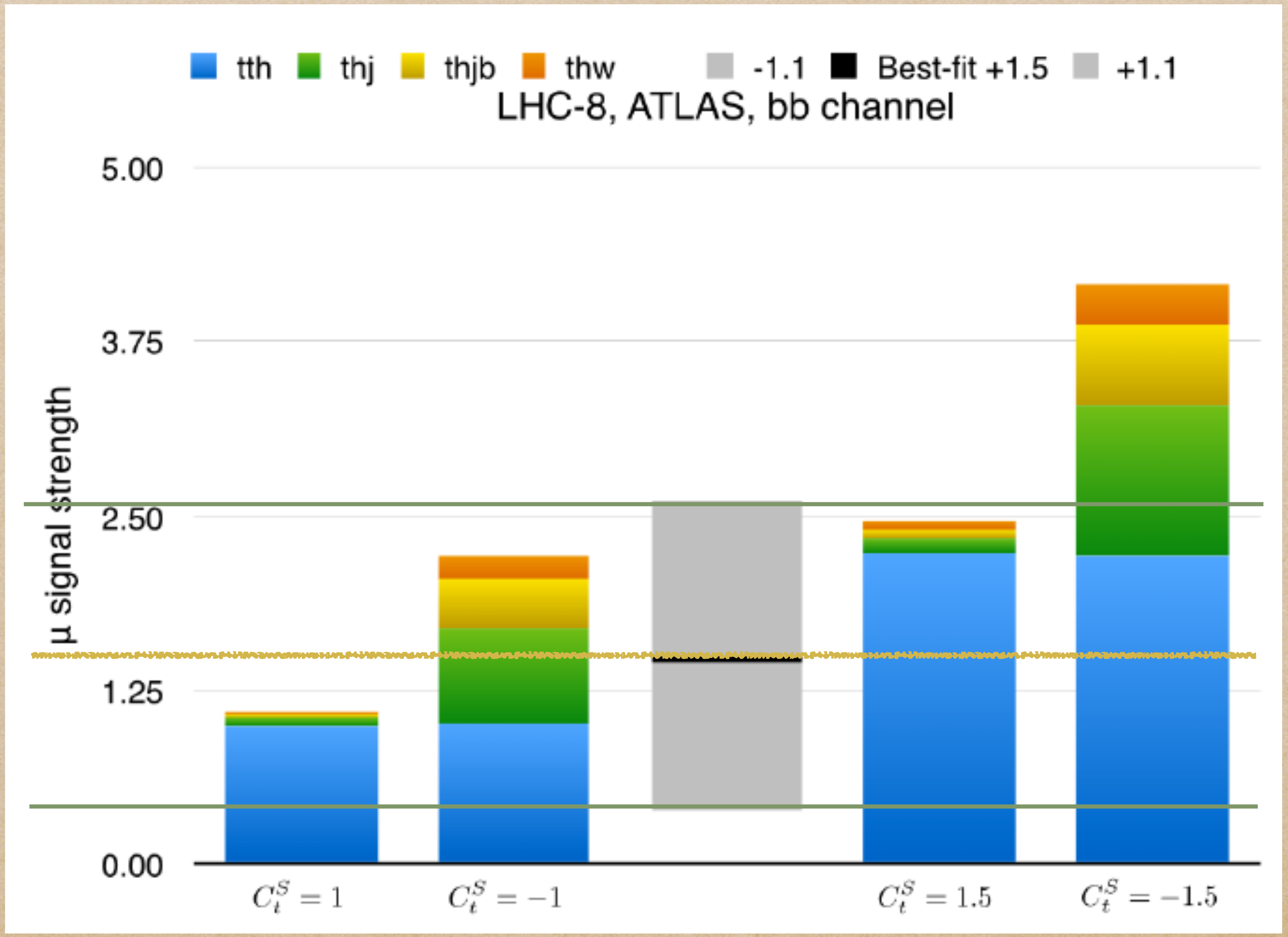

Category bb for h -> bb

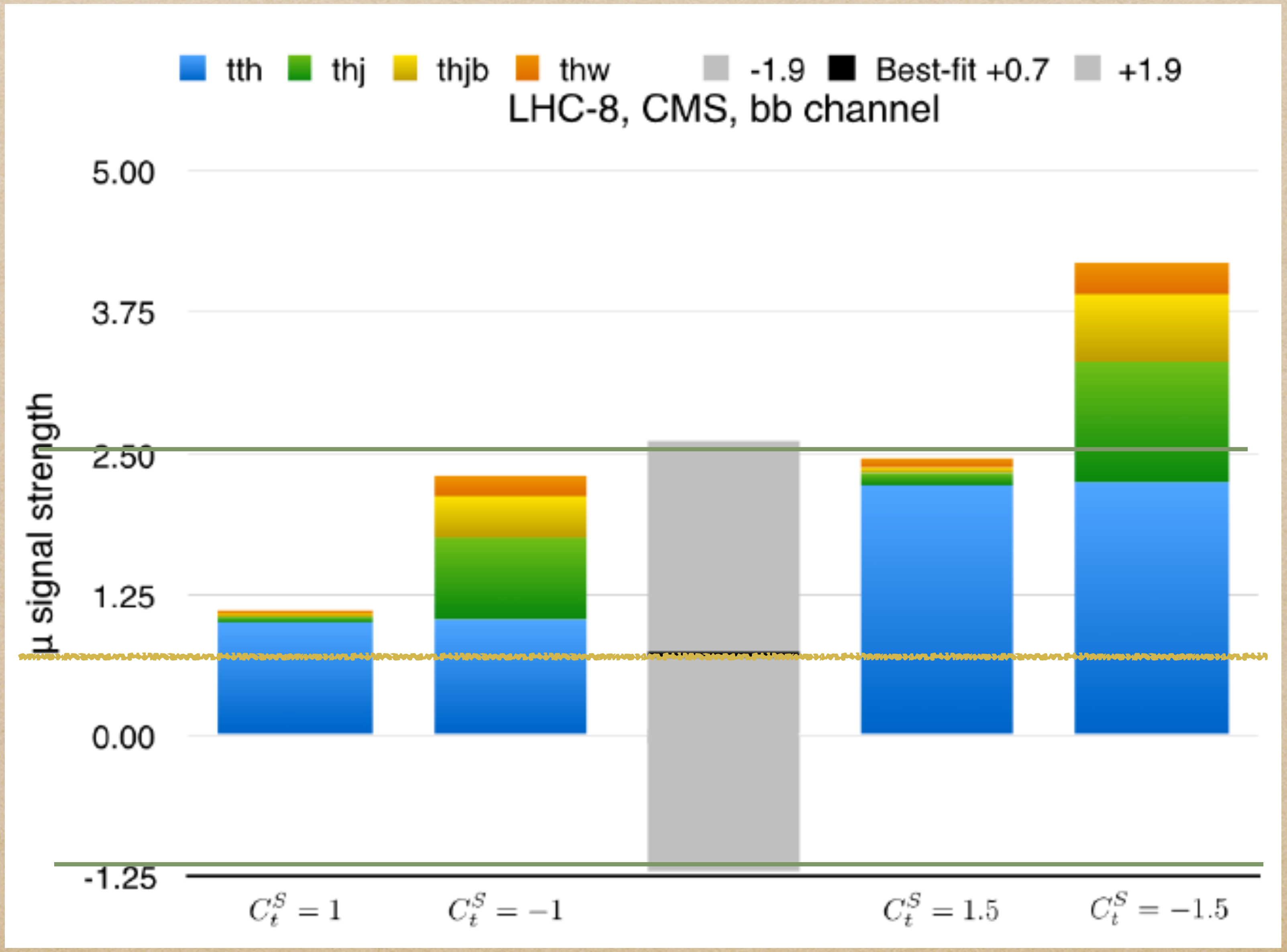

Disentangling thX from tth

C^S_t=1 C^S_t=-1 C^S_t=1.5 C^S_t=-1.5

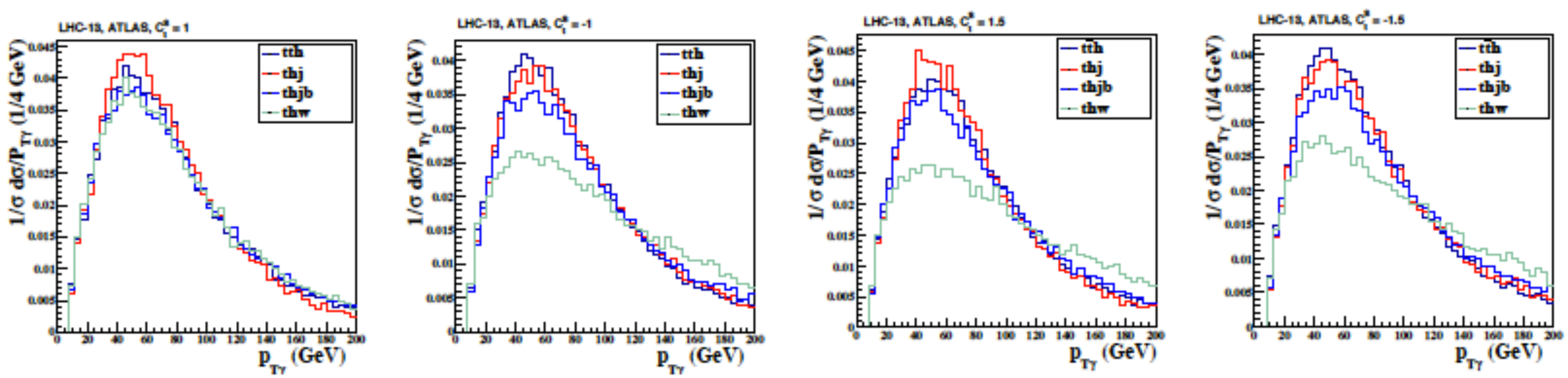

FIG. 8. The P_{T_γ} distributions for the $t\bar{t}h$ and thX processes in the $h \to \gamma\gamma$ channel at LHC-13 taking $C_t^S = +1, -1, +1.5, -1.5$ from left to right. We use the Delphes ATLAS template for detector simulations.

We can separate thW from tth

the thW process has a harder p_T photon

Disentangling thX from tth

C^S_t=1 C^S_t=-1 C^S_t=1.5 C^S_t=-1.5

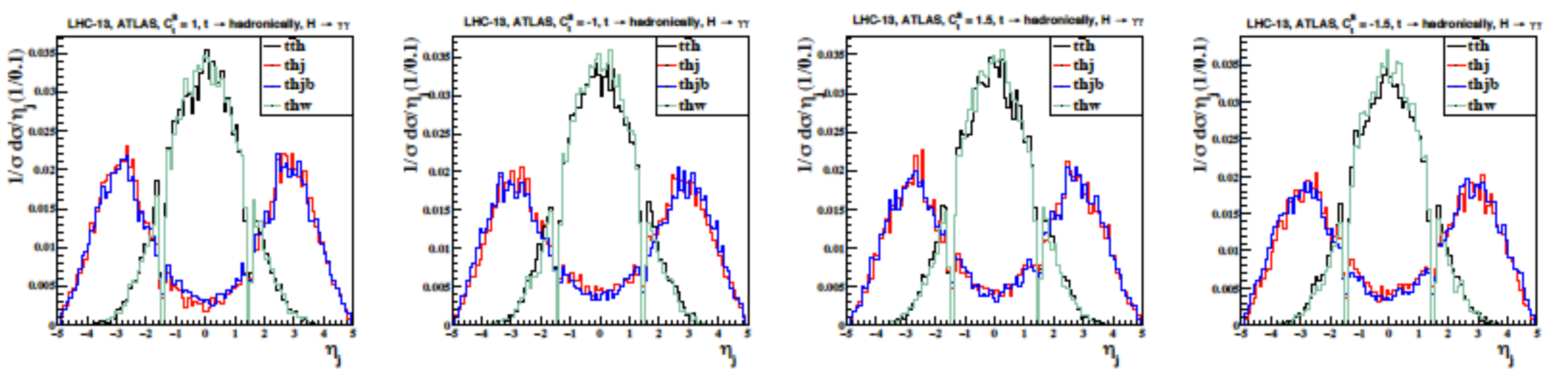

FIG. 9. The same as in Fig. 8 but for the η_j distributions.

We can separate thj, thjb from tth

The dominant thX processes are thj and $thjb$, both of which contain a very forward energetic jet.

Conclusions

- In this work, we have demonstrated explicitly that the thX processes can significantly increase the experimentally measured signal strength mu(tth) when the relative sign of the top-Yukawa coupling to the gauge-Higgs coupling is reversed.
- The signal strengths can be as large as 2-4 in the category Leptons for h -> multileptons, 7-13 in the category diphoton for h -> diphoton, and 2-4 in the category bb for h -> bb.
- When more data are collected at 13 TeV, we can choose more specific cuts to single out the thX processes, which can effectively determine the size and the sign of the top-Yukawa coupling.

CMS search for the Associated Higgs production with a Single Top Quark

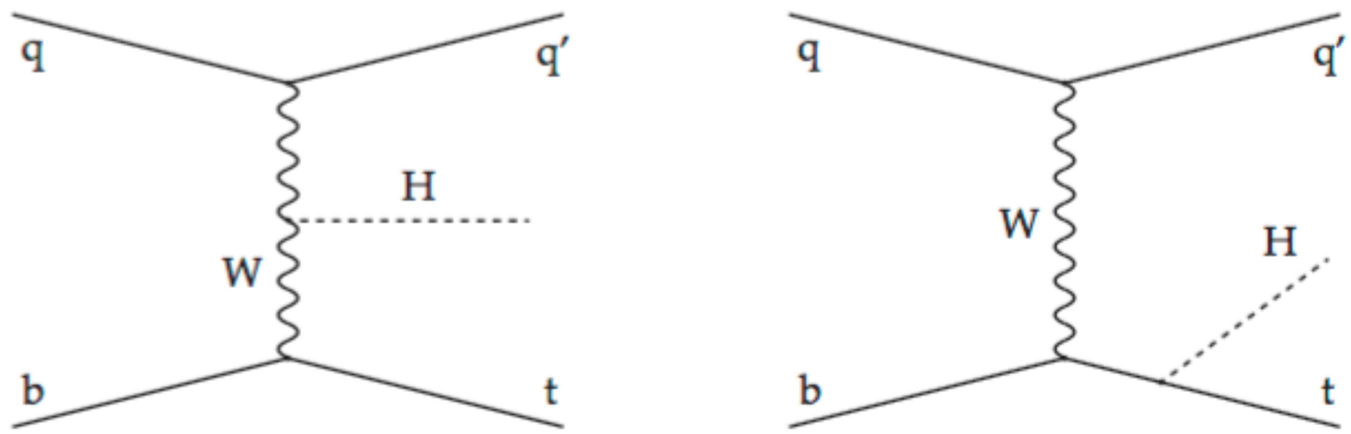

Figure 1: Dominant Feynman diagrams for the production of tHq events: the Higgs boson is typically radiated from the heavier particles of the diagram, i.e. the W boson (left) or the top quark (right).

arXiv:1509.08159

JHEP 1606 (2016) 177

CMS search for the Associated Higgs production with a Single Top Quark

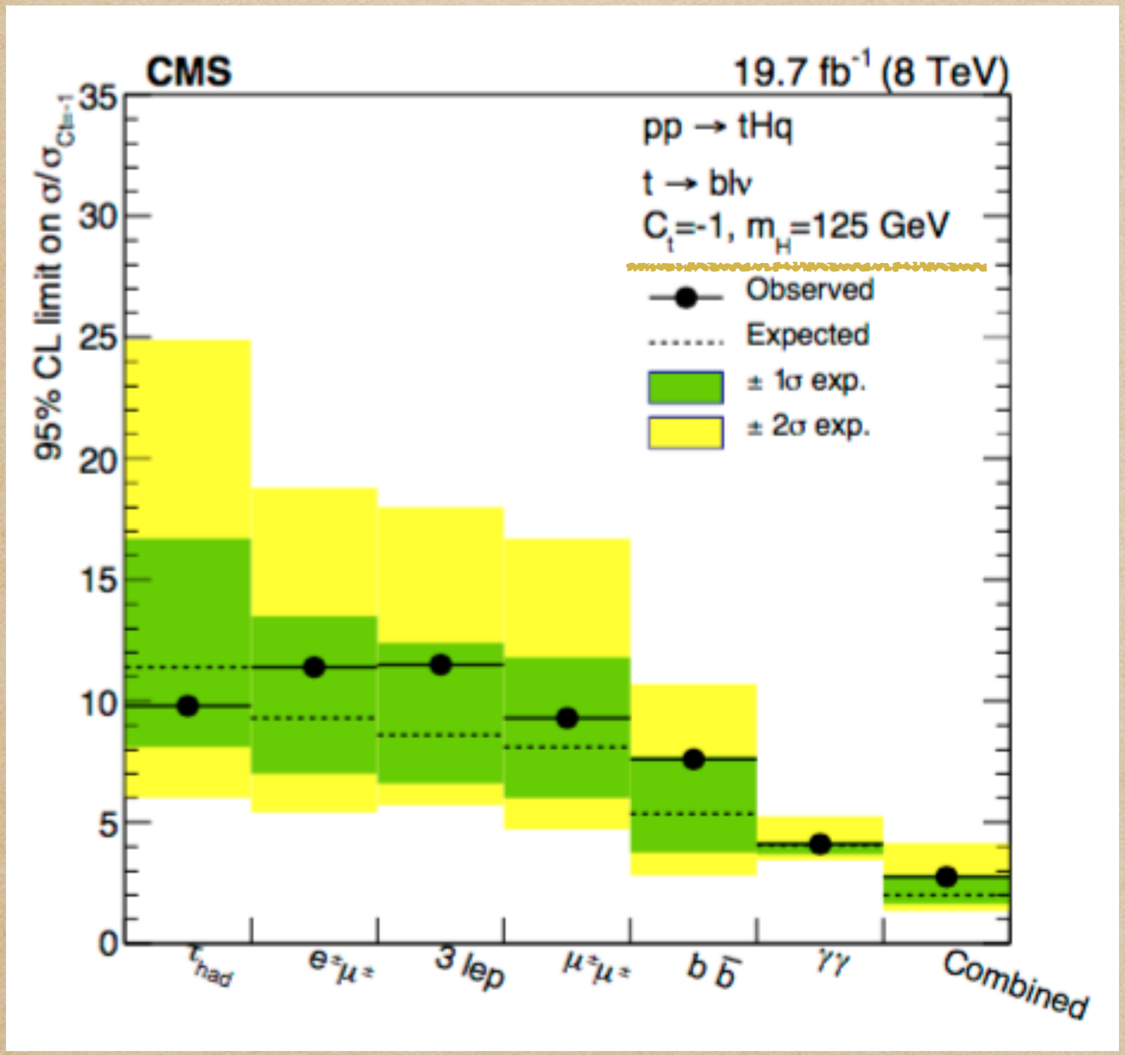

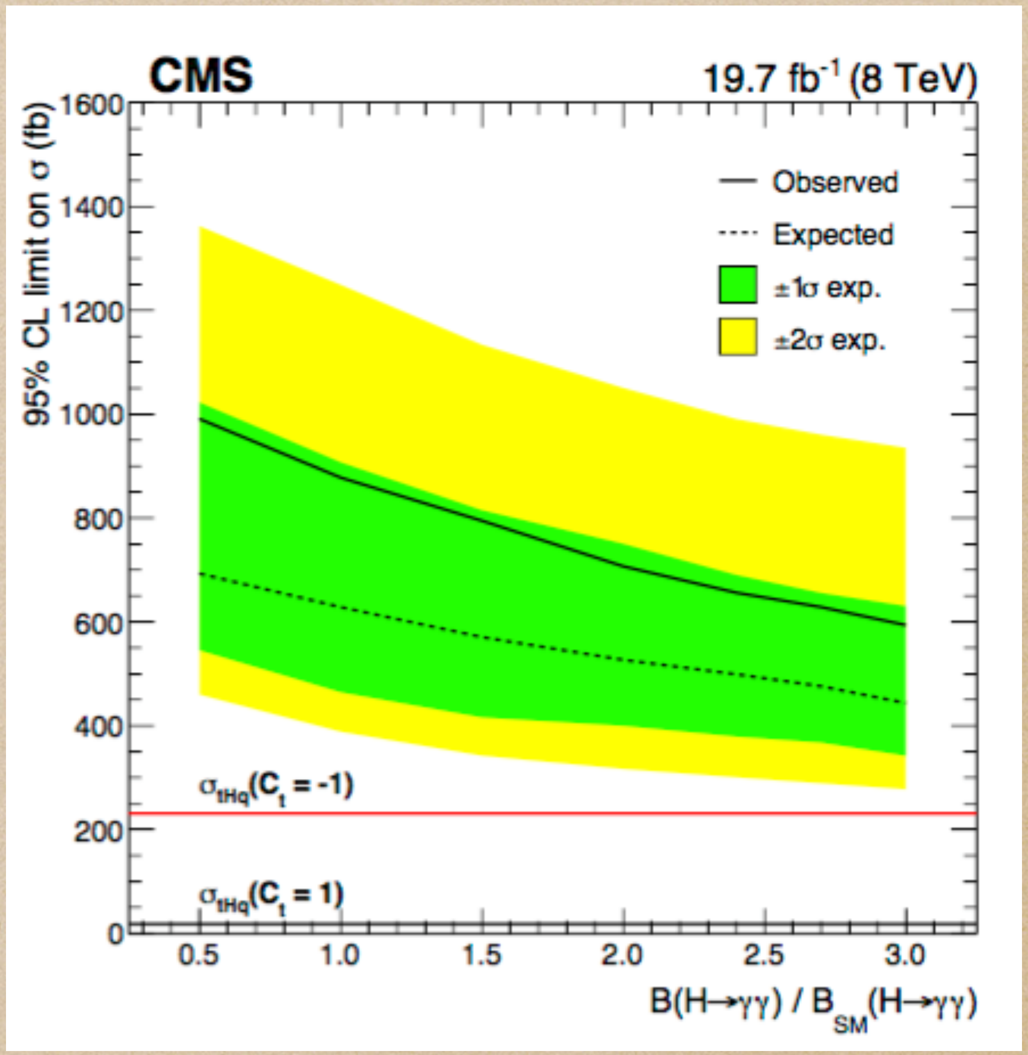

JHEP 1606 (2016) 177

arXiv:1509.08159

- It is time to pin down both the Sign and Size of the Top-Yukawa Coupling at the LHC NOW ! !

Thank You For Your Attention ! !